

Interfacing Multi-Megawatt Large Scale Offshore Wind Turbine with modular multilevel converter

Kateryna Morozovska

30.11.2015



Interfacing Multi-Megawatt Large Scale Offshore Wind Turbine with modular multilevel converter

MASTER OF SCIENCE THESIS

For obtaining the degree of Master of Science in Electrical
Engineering at Delft University of Technology and in
Technology-Wind Energy at Norwegian University of Science and
Technology.

Kateryna Morozovska

30.11.2015

European Wind Energy Master - EWEM
Delft University of Technology
Norwegian University of Science and Technology



Copyright © Kateryna Morozovska
All rights reserved.

EUROPEAN WIND ENERGY MASTER - EWEM
OF
ELECTRICAL POWER SYSTEMS TRACK

The undersigned hereby certify that they have read and recommend to the European Wind Energy Master - EWEM for acceptance a thesis entitled **“Interfacing Multi-Megawatt Large Scale Offshore Wind Turbine with modular multilevel converter”** by **Kateryna Morozovska** in partial fulfillment of the requirements for the degree of **Master of Science**.

Dated: 30.11.2015

Supervisor:

prof.dr.ir. Elisabetta Tedeschi of NTNU

Supervisor:

prof. Pavol Bauer of TU Delft

Reader:

Phd Gilbert Bergna-Diaz of NTNU

Summary

The aim of the master thesis was to investigate the effect of Modular Multilevel Converter (MMC) on wind energy electrical system. In different literature sources MMC is used at the grid side of the turbine. This thesis has a focus on the implementation of the MMC at the generator side of the wind turbine and comparing this new topology with already existing ones. Not only the advantages, but also the complications that arise when trying to design control strategy for this topology, are described in this thesis.

The reader is introduced with the general structure and operation of MMC. The paper also gives a brief overview of the wind turbine structure and different electrical systems that can be possibly used for wind energy production.

The simulation of the wind energy electrical system is carried out using MatLab Simulink. The simulation model contains permanent magnet synchronous generator (PMSG) and two MMC's, one at generator side and one at the grid side. A big part of the master thesis is a description of the control of the generator and the converter.

Conclusions compare the obtained results during simulations with the already existing topologies, that have been studied by student during 2 year master program.

Acknowledgements

I would like to thank the following people who guided me during my studies of European Wind Energy Masters and work on my master thesis.

prof. Elisabetta Tedeschi and Phd Gilbert Bergna-Diaz, my supervisors, whom I should thank for encouragement, guidance and support.

EWEM coordination group (Linda, Zarah, Carlos, Henk, Olav) for giving students an opportunity to study Wind Energy at the best European Universities and guiding them throughout their studies.

My friends and colleagues Dimitris and Emre for interesting discussions and support.

To my new working team for being flexible with my schedule and support during the last months.

To my mother Tatiana for giving me this amazing opportunity to study, even during the hardest times my country ever experienced.

Delft, The Netherlands
30.11.2015

Kateryna Morozovska

Contents

Summary	v
Acknowledgements	vii
List of Figures	xii
List of Tables	xiii
1 Introduction	1
1.1 State of the art	1
1.2 Objectives	2
1.2.1 General objective	2
1.2.2 Specific objectives	2
1.3 Layout of the thesis	2
Nomenclature	1
2 A brief introduction to Wind Energy generation	5
2.1 Wind power conversion. Electrical components of wind turbines.	6
2.2 Wind turbine drive train types. Advantages and disadvantages.	8
3 Overview of different wind turbine system configurations	11
3.0.1 General description of full-scale converter	12
3.0.2 Full-scale converter. Overview of existing solutions	13
3.0.3 Two-level back-to-back inverter	14
3.1 Permanent Magnet Synchronous Generator	15
3.1.1 Calculation of power and torque of the PMSG	17

4	The Modular Multilevel Converters	19
4.1	Introduction	19
4.2	Sub-module operation principles	21
4.2.1	Balancing Algorithm	22
4.2.2	Operation of the MMC converter	23
4.2.3	Mathematical modeling of MMC	27
4.3	Determination of parameters of the semiconductor devices	28
5	Control of the wind turbine	31
5.1	Review of the system structure	31
5.2	Control of permanent magnet synchronous generator	32
5.2.1	Modeling of drive train	32
5.2.2	Modeling of PMSG	32
5.3	Control of the two-level inverter	33
5.4	Control of the MMC	34
5.4.1	Different modulation techniques for MMC	34
5.4.2	Control of the MMC's outer loop energy dynamics	37
5.4.3	Circulating current control	37
5.4.4	Control of the generator side MMC	38
6	Simulation and Results	39
6.1	General structure	39
6.2	Generator side	39
6.2.1	Simulation of the wind turbine in MatLab Simulink	39
6.2.2	PMSM simulatin parameters estimation	41
6.3	Simulation of the Modular Multilevel Converter	42
6.3.1	Parameter estimation of the Main MMC components	42
6.3.2	Balancing algorithm	43
6.4	Control of output parameters	44
6.4.1	Output of the converter control	46
6.5	Simulation of IFOC for PMSG interfaced with two-level inverter	50
7	Discussion. Conclusion. Future work	53
	References	55
A	Calculation of converter parameters	59
B	Balancing algorithm for one arm of the converter	61
C	Space Vector Modulation script	63

List of Figures

2.1	Wind Energy Market forecast for 2014-2019.	5
2.2	Growth in size of the rotor diameter of wind turbines since 1980.	6
2.3	Wind power conversion model.	6
2.4	General placement of electrical components in the nacelle.	8
2.5	Schematic drawing of four different generator systems.	8
3.1	Wind Turbine interfaced with Doubly Fed Induction Generator with the back-to-back converter connected to the rotor.	11
3.2	Wind Turbine with full-scale back-to-back converter.	12
3.3	Wind Turbine System with Diode-Bridge rectifier and boost converter. . .	13
3.4	Wind power conversion system using two-level back-to-back Voltage Source Inverter.	13
3.5	Wind power conversion system using modular multilevel converter.	14
3.6	3-phase two level Voltage Source Inverter.	15
4.1	One leg of 3phase MMC.	20
4.2	Two types of submodule configuration.	20
4.3	Active states of submodule operation. Where blue is for current flowing in positive direction and red is for current flowing in negative direction. . . .	21
4.4	Bypassed states of submodule operation. Where blue is for current flowing in the right direction and red is for current flowing in opposite direction. .	22
4.5	Blocked state. Both IGBT's are open.	22
4.6	Equivalent circuit for normal operation using Ideal Switching devices. . .	23
5.1	Schematic representation of back-to-back MMC for the Wind turbine. . .	31
5.2	Indirect Field-oriented Control of PMSG.	33
5.3	1DM modulation algorithm for one phase of the converter.	36
5.4	Energy sum control scheme.	37

5.5	Energy difference control scheme.	37
6.1	MatLab Simulink model for the simulation of the 10 MW wind turbine with back-to-back MMC converter.	40
6.2	Wind Turbine and Wind Turbine Generator part of MatLab Simulink model.	41
6.3	MatLab Simulink Wind turbine block and it's mask structure.	41
6.4	MatLab Simulink block parameters for Permanent Magnet Synchronous Generator (PMSG).	42
6.5	Generator side and grid side MMC converters	43
6.6	Balancing algorithm for both generator and converter side converters.	44
6.7	Successful implementation of balancing algorithm.	44
6.8	Signal modulation blocks for both MMCs	45
6.9	Control blocks for both generator side and grid side converters.	45
6.10	Output waveforms of the circulating and output MMC currents for the grid side converter.	46
6.11	3 phase output currents and voltages measured at the grid side.	46
6.12	Comparison of outer loop and inner loop control outputs for converter gate signal generation.	47
6.13	Output voltage signal from the PI converter.	47
6.14	Voltages driving grid currents in pu.	48
6.15	Voltages driving grid currents in pu.	48
6.16	Voltage driving the circulating current before the PI control.	49
6.17	Voltage driving the circulating current after the PI control.	49
6.18	PMSG with two level inverter. Speed regulator and indirect field oriented control.	51
6.19	d-q axes currents and torque regulation.	52

List of Tables

2.1	Comparison of four wind turbine generator concepts: + strength, - weakness.	9
5.1	3 Phase system equations determining switching sequence and switching times by 1DM modulation principle.	36
6.1	Input parameters of Permanent Magnet Synchronous Generator (PMSM).	42
6.2	MMC submodule calculated input parameters	43

Chapter 1

Introduction

For last decades renewable energy generation has become an important part of electricity production. Market share of renewables in Europe and worldwide is rising each year. Wind energy has a big share in renewable energy capacity nowadays.

According to the Numbers from Global Wind Energy Council [1] in 2014 there were 51.5 GW of installed wind power, that number beats all the previous records and brings cumulative installed global capacity to the number of 369.6 GW and approximate number of wind turbines in operation to 268,000. Also wind energy helped to avoid over 608 million tonnes of CO₂ emissions globally.

By the end of 2014 3% of the global electricity demand was covered by wind energy. As for the European Union(EU) the wind energy covers around 10,2 % of the total electricity consumption. Considering current active plans about development of wind energy it can be estimated that the global share of wind energy in the power market will increase up to 17-19% by the end of 2030 [1].

Wind energy is very effective solution, average wind turbine needs from 3 to 6 months to compensate the energy used for it's production, operation and recycling after decommissioning. If compare generation-consumption rate of wind power with nonrenewable energy sources the nuclear plant generates 16 times more power then it consumes, the coal plant 11 times more and for the wind power this number is from 17 to 39[1].

1.1 State of the art

Very important stage of every research is literature study on topic and review of already existing solutions. The reference list of these report is quite diverse, but there were several papers and reports that influenced my work the most.

The concept of the Wind Turbine interfaced with Modular Multilevel Converter MMC was described in paper "Device Loading of Modular Multilevel Converter MMC in Wind Power Application" [2]. That work gave an idea about the advantages that wind turbine can gain with the use of advanced multilevel converter. On the other side it gave an idea that it could be interesting to investigate which advantages and disadvantages can be seen

if interfacing the wind turbine with two MMC converters. The energy analysis performed in this paper shows that MMC with even low number of submodules requires lower rated current compared to two-level converter for the same rated power application. It is also proved by the loss distribution model that for equal loss distribution between submodules a special selection mechanism should be used. It is also proved that for the low power applications the requirement for extra reactive power input can lower the efficiency and has unequal loss distribution [2].

A great influence on the design of control during simulation process and also understanding the MMC working principle in general was made by the PhD Thesis "Modular Multilevel Converter Control for Multi-terminal HVDC Operation" [3] and also several papers related to that research [4], [5]. The control strategy described in that thesis was later used for control of the grid side converter, and also modified to control the generator side MMC.

1.2 Objectives

1.2.1 General objective

The main objective of this thesis is to develop an effective solution for power conversion for large scale wind turbine using modular multilevel converter.

1.2.2 Specific objectives

- To develop a Matlab Simulink model of large scale wind turbine interfaced with back-to-back 2-level inverter and permanent magnet synchronous generator.
- To develop control strategy of the given turbine using PID controller.
- To replace the back-to-back 2-level inverter with a modular multilevel converter.
- By means of PID control minimize the harmonic component of the current, caused by reactive power injection and also regulate the generator speed to keep power production at nominal value. Make sure that resulting control strategy is frequency adaptive. To balance capacitors in converter arms, controlling the frequency of the arms current.
- To compare pros and cons of the following technical solutions.
- To proof the benefits of interfacing offshore wind turbines with MMC.

1.3 Layout of the thesis

The thesis is subdivided into following chapters:

-
- Chapter 1 is a brief introduction to the report. It includes short literature overview, main objectives described in the thesis as far as problem definition and reasoning for the importance of current work.
 - Chapter 2 is a brief description of wind energy technology and review of future trends in wind energy.
 - Chapter 3 describes the drive train structure of modern wind turbine. A review of different electrical systems for wind turbines.
 - Chapter 4 is general introduction to MMC topology. The converter operation, construction and control strategy are described.
 - In Chapter 5 describes proposed control scheme for the wind turbine interfaced with back-to-back MMC converter.
 - Chapter 6 is the detailed description of the MatLab Simulink the implementation of all the theoretical knowledge described in previous chapters, results of simulations and their comparison.
 - Chapter 7 is the discussion on the results and comparison the results with the information on wind turbines interfaced with two level converters from the literature. Conclusions on the performed work and suggestions for future tasks in the area.

Chapter 2

A brief introduction to Wind Energy generation

This section gives a brief explanation of wind power conversion and general structure of the wind turbine as well as presents different drive train solutions. It concludes with the reasoning of the choice of particular drive train solution for current application.

Wind energy production keeps being very promising industry. According to the GWEC Global Status Overview, in 2014 the annual wind energy market grew by 44 % and for the first time in the history passed point of 50 GW of yearly installed capacity [6]. At the end of 2014 the global total installed capacity equaled to 369,6 GW [6].

Also, as is shown on the figure 2.1, by the year 2019 the Global cumulative installed capacity is expected to grow up till 600 GW [7]. An increasing demand in installed



Figure 2.1: Wind Energy Market forecast for 2014-2019 [7].

capacity also requires new engineering solutions, which can provide wind turbines of higher production capability, increased safety, efficient power solutions and fairly better economy. From the Figure 2.2 we can clearly see that wind turbines tend to grow in size. And together with the size, the production capacity of turbine rises, because the mechanical energy transferred to the generator is directly proportional to the rotor swept area [8].

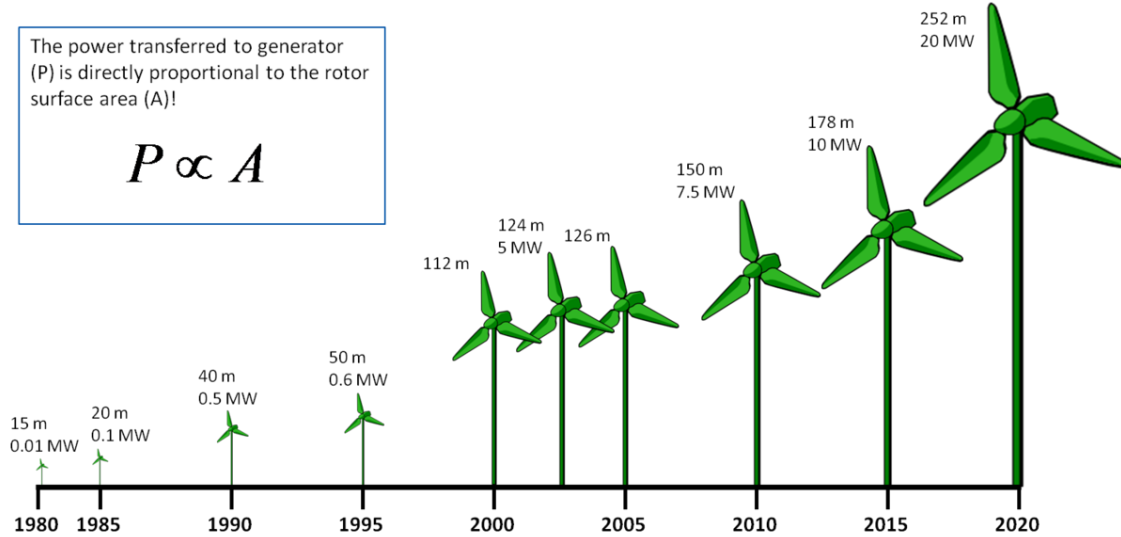


Figure 2.2: Growth in size of the rotor diameter of wind turbines since 1980 [9].

2.1 Wind power conversion. Electrical components of wind turbines.

A wind turbine is a structure that is ment to transfer kinetic energy extracted from the wind into rotational energy at the shaft and then into electrical energy in the generator. [10] Wind power extraction is shown on the Figure 2.3

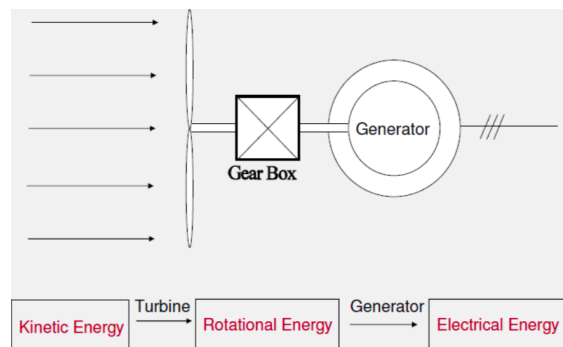


Figure 2.3: Wind power conversion model [11].

The kinetic energy from the wind that moves wind turbine blades can be derived from

the equation 2.1 [12]. [10].

$$E_k = \frac{1}{2}mV^2 \quad (2.1)$$

Using 2.1, the instantaneous power captured by turbine, can be calculated according to 2.2 [12]

$$P_{wind} = \frac{1}{2}\rho SV^2 \quad (2.2)$$

One of the key parameters of wind power production is the power coefficient C_p . The value of power coefficient depends on the design of wind turbine and its orientation with respect to the wind direction. By its definition, C_p is the ratio between power extracted from the wind P_{wind} and power available at generator shaft P_{el} as shown in the equation 2.3 [12] [10].

$$C_p = \frac{P_{el}}{P_{wind}} \quad (2.3)$$

The theoretical maximum $C_p = 16/27 = 0.593$ and is called Betz limit. In real life applications C_p usually varies between 0.4-0.5 [10].

The general equation for the available power at the generator shaft is:

$$P_w = \frac{1}{2}\rho C_p A V^3 \quad (2.4)$$

where ρ is the air density $\rho = 1.225 \text{ kg/m}^3$; A is the cross-sectional area; which is equal to rotor swept area and V is the wind speed in m/s.

C_p can also be defined as a function of tip speed ratio $C_p = f(\lambda)$. Where λ is defined by the formula 2.5.

$$\lambda = \frac{R\omega}{V} \quad (2.5)$$

where R is the radius of rotor swept area and ω is the angular speed. Power coefficient can also be represented as polynom of 6th order in the expression 2.6 [12].

$$C_p = (a_0 + a_1\lambda + a_2\lambda^2 + a_3\lambda^3 + a_4\lambda^4 + a_5\lambda^5 + a_6\lambda^6) \cdot \lambda \quad (2.6)$$

The Figure 2.4 gives a brief understanding of the placement of the main electrical parts of the wind turbine. Most of the devices, taking part in energy conversion are placed on top of the wind turbine tower, that part is called nacelle. The nacelle consists of wind turbine rotor with connected blades, hub, generator, gear-box, transformer and power converter. The combination of components may vary depending on different applications.

In given research project the main focus is on large scale wind turbines. To make the model more suitable for current wind energy market the 3-bladed 10MW wind turbine is used. The 3-bladed turbines are the most popular solution nowadays. The efficiency-cost relation is optimal as well as visual ergonomics. The offshore wind turbines are usually of large-scale power from 3.6MW and higher, the most common installed offshore capacity is either 3.6 MW or 5 MW, but evaluating the tendency of wind turbine capacity growing, the wind turbine used in this paper been assigned the capacity of 10 MW.

Mechanical and electrical components of the nacelle form drive train of the wind turbine. Wind turbine drive train mainly consists of following components: shaft, gear-box, generator, converter, transformer. With the growing wind turbines power the size and weight of the nacelle becomes an essential topic.

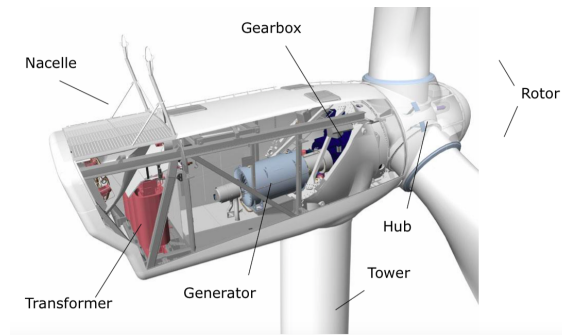


Figure 2.4: General placement of electrical components in the nacelle [13].

2.2 Wind turbine drive train types. Advantages and disadvantages.

Wind turbine drivetrain has developed a lot with years. In the past years, the wind energy conversion systems (WECS) were of the fixed speed and used stall control to regulate the energy input. After development of double-fed induction generators and wound-rotor induction generators, variable speed WECS took over [14].

There are 4 commonly used types of generator systems [15]. All 4 types are shown on the Figure 2.5. Comparison of most popular generator systems is shown in the Table

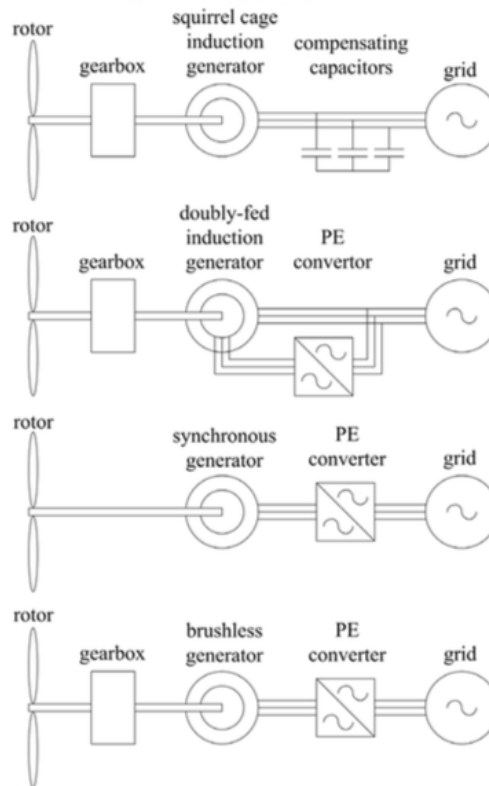


Figure 2.5: Schematic drawing of four different generator systems [11].

Table 2.1: Comparison of four wind turbine generator concepts: + strength, - weakness[15].

		CS	DFIG	GFC	DD
Cost, size and weight		+	+/-	+/-	-
Suitability for 50 and 60 Hz grid		-	-	+	+
Audible noise from blades		-	+	+	+
Energy yield	Variable speed	-	+	+	+
	Gearbox	-	-	-	+
	Generator	+	+	+	-
	Converter	+	+/-	-	-
Reliability and maintenance	Brushes	+	-	+	-(PM: +)
	Gearbox	-	-	-	+
	Mechanical loads	-	+	+	+
	Complexity	+	-	-	-
Power quality	'Flicker'	-	+	+	+
	V&f control possible	-	+	+	+
	Harmonics	+	-	-	-
Grid faults	Fault currents	+	-	-	-
	Fault ride-through	+	+/-	+	+
	Restoring voltage	-	+/-	+	+

2.1. Using the following comparison it is possible to conclude that for large scale offshore application DD generator system is the most suitable. As far as the focus of the thesis is on the high voltage; large capacity wind turbine; situated offshore, the maintenance plays an important role. Providing sufficient and fast maintenance of the offshore wind farm is more time consuming and more complicated as compared to the onshore. The wind turbine will be interfaced with Permanent Magnet Synchronous Generator (PMSG), the advantages of PMSG compared to the other generators are:

- high efficiency
- elimination of field losses
- comparatively small size, due to use of high number of pole pairs.
- high reliability, good for applications off-shore or rural onshore areas [16].

As a disadvantage could be stated the cost of permanent magnets. But this disadvantage becomes less valuable in high power applications.

For the current research DD (Direct Drive) generator with full converter was chosen. As far as current research has its main focus on operation of the converter, so the drivetrain concepts with gear box will only add additional calculations.

Overview of different wind turbine system configurations

It has been mentioned earlier that the energy conversion process in wind turbine is done in 3 steps: kinetic energy of the wind is captured by blades and transformed to the mechanical energy at generator shaft; then mechanical energy is transformed into electrical energy by the generator; and the last step is power being delivered from the generator to the grid. The first step is usually done in the same way for all the turbines, with the only possible change - using or not using the gear box. The second and third stages can have significant differences from one turbine to another depending on the configuration. The first commercial configuration was introduced in Denmark in late 1970's and it got the name 'Danish concept'. 'Danish concept' is a fixed-speed induction generator directly connected to the grid [17]. With the development of Wind Energy Technology the need in variable-speed configurations have become essential for the improving the power quality. In 1990's Doubly Fed Induction Generator(DFIG) was introduced, DFIG concept is variable-speed and interfaces the grid through the power converter that is connected to the rotor as is shown on the Figure 3.1.

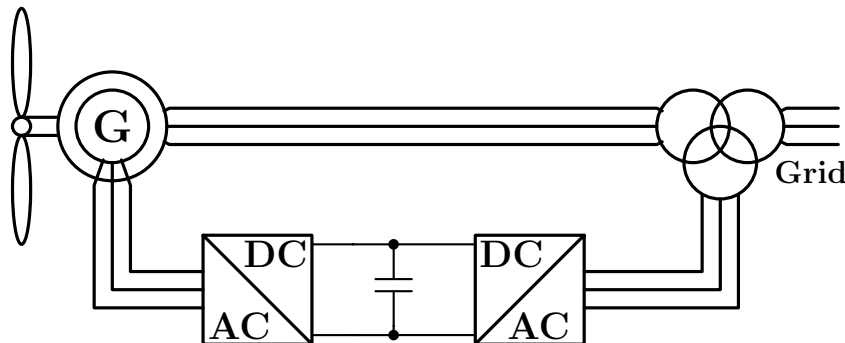


Figure 3.1: Wind Turbine interfaced with Doubly Fed Induction Generator with the back-to-back converter connected to the rotor.

The use of power converter allows to partially control active and reactive power that is injected into the grid. Although DFIG concept is used also nowadays, its power generation capacity is limited. DFIG is scaled up to 5 MW, but for high power applications there is a need of another solution [17] [18].

The solution for high power applications was introduced by Siemens and Enercon in 2000's. New configuration of the wind turbine system was interfaced with full-scale converter (FCS) with synchronous generator on the Figure 3.2. Full-scale power converter configuration implies complete control of the conversion process and minimization of current harmonics [18]. One of the drawbacks of such a system is the cost power electronic components, but on the other side full-scale converter provides higher system efficiency and requires less maintenance, so this solution can be of a particular interest for the applications in isolated areas, like offshore wind farms or onshore wind farms situated in rural areas.

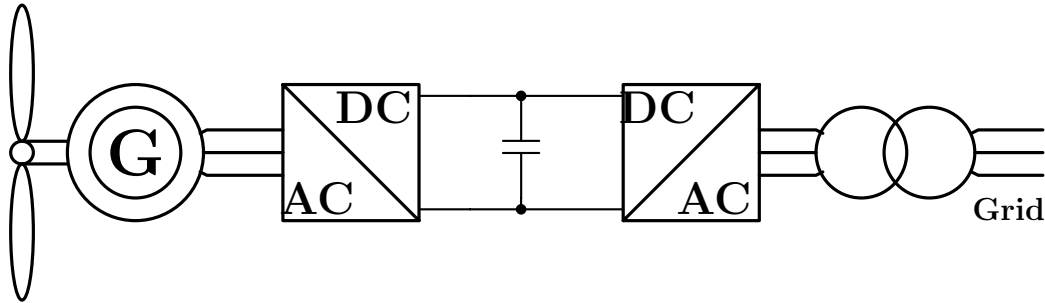


Figure 3.2: Wind Turbine with full-scale back-to-back converter.

The converter part of wind turbine system is of greater interest in this thesis, so at the beginning different concepts of FSC's will be introduced to this report.

3.0.1 General description of full-scale converter

The FSC Wind Turbine System (WTS) requires use of two converters as it is shown on the Figure 3.2. Generally converters can be categorized as:

- Two level converters
- Multilevel converters
- Tandem converters
- Resonant converters
- Matrix converters [18].

FSC gives reactive power compensation and smooth connection to the grid [19].

3.0.2 Full-scale converter. Overview of existing solutions

The most primitive type of FSC is a combination of diode-bridge rectifier, boost converter and two level voltage-source inverter. This topology is schematically shown on the Figure 3.3. Here the rectifier is converting the AC side current into DC output, then the boost converter is increasing voltage to the necessary level and inverter is transforming the DC input to the AC output connected to the grid. This topology is quite weak, because of the high torque-ripple from the high-current harmonic component. This topology is low cost so it can be suitable for the applications lower than 1 MW [18].

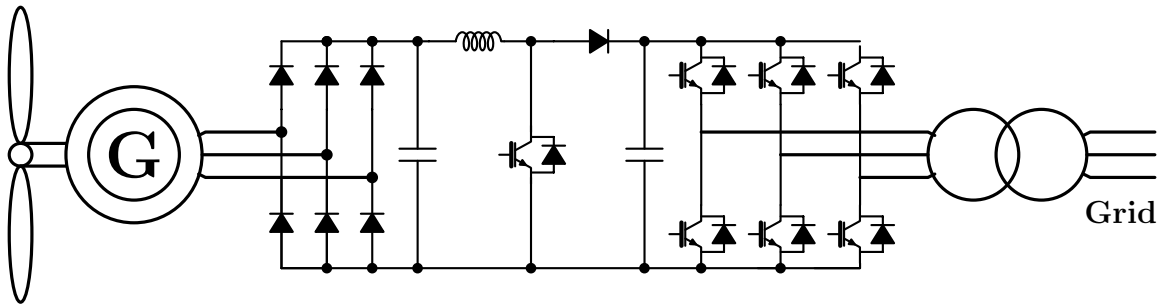


Figure 3.3: Wind Turbine System with Diode-Bridge rectifier and boost converter.

The most commonly used topology is two-level back-to-back Voltage Source Inverter (VSI) as on the Figure 3.4. Two level back-to-back VSI is basically two inverters connected through the DC link. Each inverter has 6 semiconductor switching devices: IGBT's, MOSFET's etc. The control of the converters is different. The generator side converter is responsible for the power flow and control or the generator speed. The grid side inverter is controlled to supply necessary amount of reactive power to the grid while keeping DC link voltage as constant [18]. However to reduce the harmonic component both inverters require to use filtering. Filter should be designed to be in a good balance between low harmonic input and fast dynamic system response [18]. A big advantage of the two level back-to-back VSI is relatively simple structure and few number of power electronic components. With the increasing power current topology is getting more disadvantages such as higher switching losses and lower efficiency. Another issue is relatively higher stresses on the generator and transformer in comparison with topologies described further.

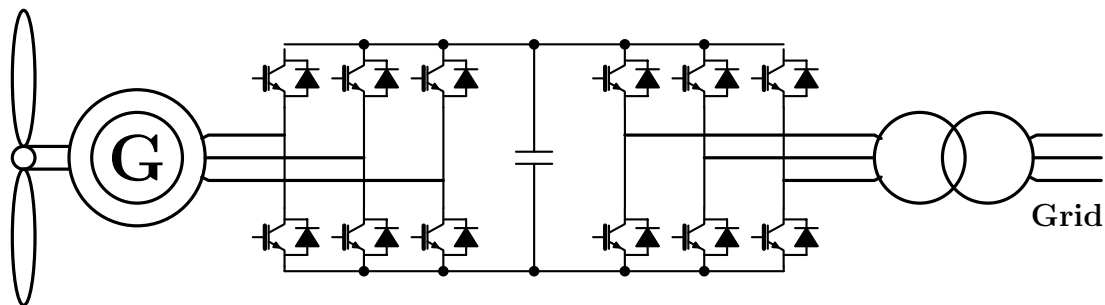


Figure 3.4: Wind power conversion system using two-level back-to-back Voltage Source Inverter.

More advanced solution is use of various multilevel converter topologies. It is possible to use following converters: Three-level (five-level) half-bridge back-to-back converter; Three-level back-to-back Neutral Point Clamped; Cascaded H-bridge Back-to-back converter with Medium-Frequency-Transformers; Multi-Cell Low Voltage Converters; N-leg diode bridge etc. I will not go into details about all the possible multilevel solutions, detailed overview can be found in the literature [18] [19] [20]. The Figure 3.5 represents scheme of the Wind Turbine System interfaced with back-to-back Modular Multilevel Converter (MMC). This exact configuration will be explained in detail in next chapters.

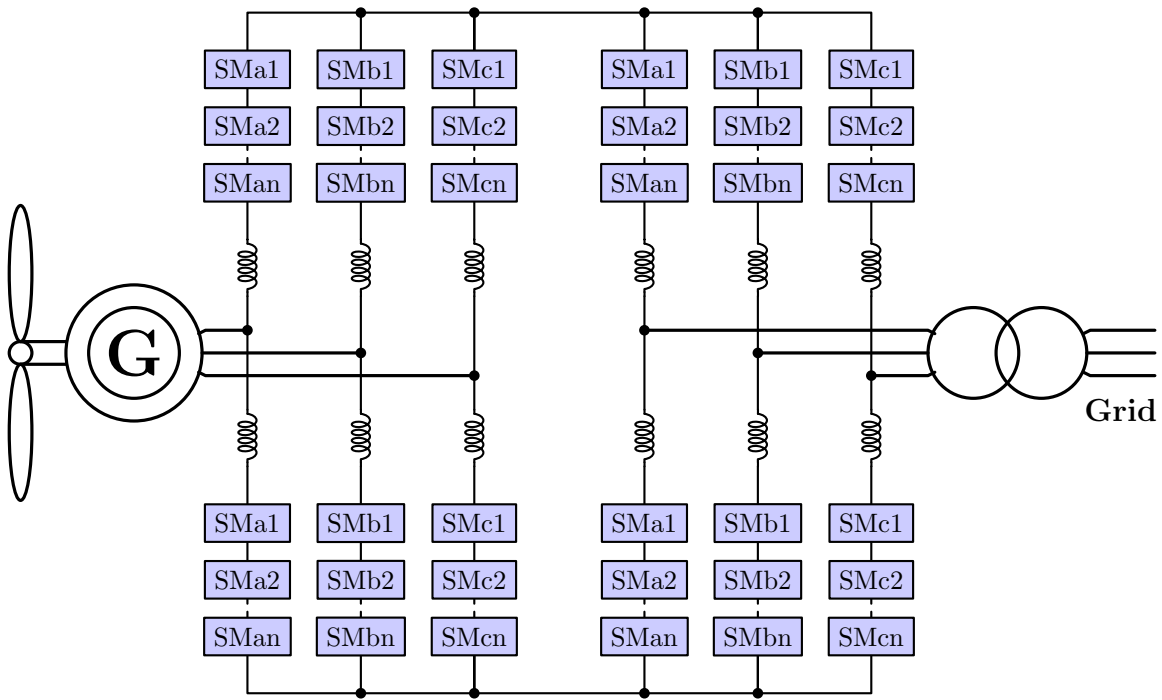


Figure 3.5: Wind power conversion system using modular multilevel converter.

3.0.3 Two-level back-to-back inverter

While the MMC will be discussed in detail in the next chapter, a little more details have to be specified about two-level voltage source inverter. Three phase voltage source inverter is in detail described in the book by Ned Mohan, Tore M. Undeland and William P. Robbins "Power Electronics. Converters, Applications, and Design." [20]. I will make a summary of the main principles of converter structure and operation. On the Figure 3.6 the construction of the inverter is drawn. Generally it consists of three legs, one for each phase; 6 semiconductor switches and 6 free-wheeling diodes. The ideal case output voltage is independent of the direction of the load current. Three-phase Voltage Source inverters are often used for uninterruptible ac power services for supply of three-phase loads, like motors or generators.

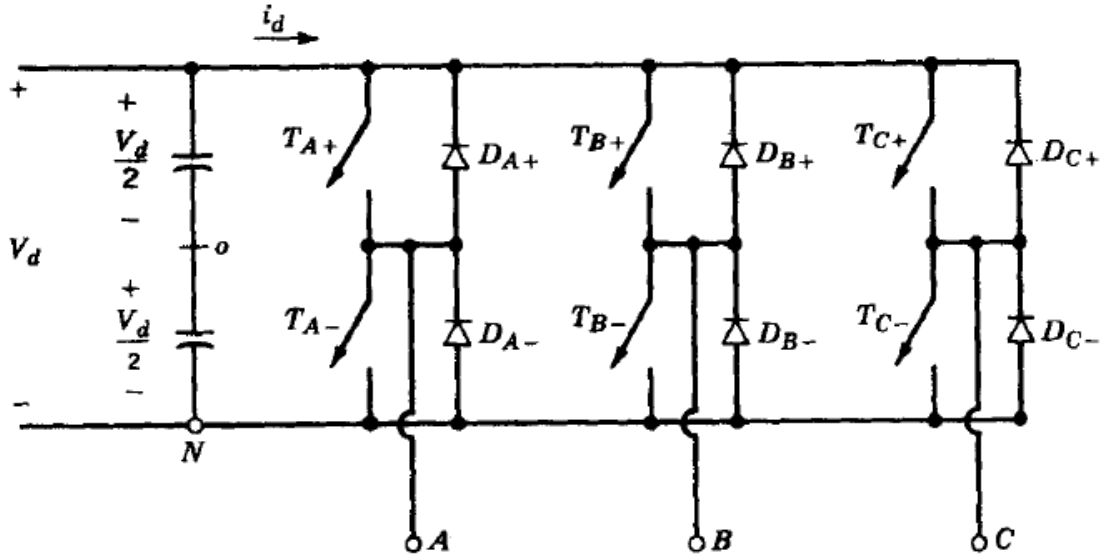


Figure 3.6: 3-phase two level Voltage Source Inverter [20].

For the control of the inverter special modulation signal should be used. Modulation signal is a tool to shape and control magnitude and frequency of the output voltage keeping the input constant. There are several different modulation techniques that can be used to control the inverter. The control signal can be square-shaped or PWM (Pulse-Width Modulation). PWM is special technique of comparing sinusoidal control voltage with the triangular voltage waveform, triangular pulse can be either in triangular shape or saw-tooth shape.

3.1 Permanent Magnet Synchronous Generator

In the following Master thesis FSC configuration with Permanent Magnet Synchronous Generator (PMSG) is studied. PMSG structure and operation principles are briefly described in the section below.

To achieve reliable simulation results the modular multilevel converter was interfaced with the generator. As have been discusses in Section 2.2 for current simulation direct drive wind turbine with permanent magnet synchronous generator (PMSG) is used. The calculation of generator parameters will be further described in this chapter.

The main focus of the thesis is the power converter performance, not the modeling of the generator, so calculations of PMSG were simplified with the following assumptions [21]:

- the damping effect in the rotor and permanent magnets is neglected
- the effect of magnetic saturation is taken into account
- the losses for hysteresis and eddy currents are neglected
- the sinusoidal back EMF is used for stator winding

- the generator equations are expressed as if for the motor

The relationship between stator currents voltages and flux linkage can be written as follows

$$\begin{bmatrix} V_{as} \\ V_{bs} \\ V_{cs} \end{bmatrix} = \begin{bmatrix} R_s & 0 & 0 \\ 0 & R_s & 0 \\ 0 & 0 & R_s \end{bmatrix} \cdot \begin{bmatrix} i_{as} \\ i_{bs} \\ i_{cs} \end{bmatrix} + \frac{d}{dt} \begin{bmatrix} \lambda_{as} \\ \lambda_{bs} \\ \lambda_{cs} \end{bmatrix} \quad (3.1)$$

where, R_s is the stator winding resistance for each phase, V_{as}, V_{bs}, V_{cs} are the instantaneous 3-phase stator voltages; i_{as}, i_{bs}, i_{cs} are instantaneous 3-phase stator currents, and $\lambda_{as}, \lambda_{bs}, \lambda_{cs}$ are instantaneous induced flux linkage per phase [22]. To obtain flux linkages following equation is used:

$$\begin{bmatrix} \lambda_{as} \\ \lambda_{bs} \\ \lambda_{cs} \end{bmatrix} = \begin{bmatrix} L_{aa} & L_{ab} & L_{ac} \\ L_{ba} & L_{bb} & L_{bc} \\ L_{ca} & L_{cb} & L_{cc} \end{bmatrix} \cdot \begin{bmatrix} i_{as} \\ i_{bs} \\ i_{cs} \end{bmatrix} + \begin{bmatrix} \lambda_r \cos(\theta_r) \\ \lambda_r \cos(\theta_r - \frac{2\pi}{3}) \\ \lambda_r \cos(\theta_r + \frac{2\pi}{3}) \end{bmatrix} \quad (3.2)$$

where, L_{aa}, L_{bb}, L_{cc} are values of self-inductance's and $L_{ab}, L_{ac}, L_{ba}, L_{bc}, L_{ca}, L_{cb}$ are the mutual between corresponding phases; the λ_r is the rotor flux linkage. All the inductance's are functions of θ_r , so it is possible to conclude that they are functions of time. To go from the 3-phase reference frame to dq0 reference frame Park's transformation is used. Park's transformation was developed in 1929 by R.H. Park for simplification of synchronous machine model analysis. The dq0 instantaneous values calculation using Park's transformation is following:

$$\begin{bmatrix} u_d \\ u_q \\ u_0 \end{bmatrix} = \sqrt{\frac{2}{3}} \begin{bmatrix} \cos(\theta_r) & \cos(\theta_r - \frac{2\pi}{3}) & \cos(\theta_r + \frac{2\pi}{3}) \\ \sin(\theta_r) & \sin(\theta_r - \frac{2\pi}{3}) & \sin(\theta_r + \frac{2\pi}{3}) \\ \frac{1}{\sqrt{2}} & \frac{1}{\sqrt{2}} & \frac{1}{\sqrt{2}} \end{bmatrix} \begin{bmatrix} u_a \\ u_b \\ u_c \end{bmatrix} \quad (3.3)$$

where u_d and u_q are instantaneous bi-phase values and u_0 is zero vector. Vectors u_{abc} and u_{dq0} can represent system voltages, currents or flux linkages.

The inverse Park's transformation makes transition from the dq0 values back to the 3phase system. Equation 3.4 represents transformation of 3phase voltages to dq0 reference frame.

$$\begin{bmatrix} u_a \\ u_b \\ u_c \end{bmatrix} = \sqrt{\frac{2}{3}} \begin{bmatrix} \cos(\theta) & -\sin(\theta) & \frac{1}{\sqrt{2}} \\ \cos(\theta - \frac{2\pi}{3}) & -\sin(\theta - \frac{2\pi}{3}) & \frac{1}{\sqrt{2}} \\ \cos(\theta + \frac{2\pi}{3}) & -\sin(\theta + \frac{2\pi}{3}) & \frac{1}{\sqrt{2}} \end{bmatrix} \begin{bmatrix} u_d \\ u_q \\ u_0 \end{bmatrix} \quad (3.4)$$

Under the balanced conditions zero vector $u_0 = 0$, so the dq0 voltage functions can be expressed as in equations 3.5 and 3.6 .

$$v_{ds} = R_s i_{ds} + L_d \frac{di_{ds}}{dt} - \omega_e L_q i_{qs} \quad (3.5)$$

$$v_{qs} = R_s i_{qs} + L_q \frac{di_{qs}}{dt} + \omega_e L_d i_{ds} + \omega_e \lambda_r \quad (3.6)$$

where, v_{ds}, v_{qs} are the stator voltages, i_{ds} and i_{qs} are stator currents, L_d and L_q are inductance's and ω_e is the electrical angular speed of the rotor; λ_r is the peak value of

rotor flux linkage.

And flux equation for the $dq0$ system:

$$\lambda_d = L_d i_d + \lambda_r \quad (3.7)$$

$$\lambda_q = L_q i_q \quad (3.8)$$

3.1.1 Calculation of power and torque of the PMSG

The 3phase power expression for permanent magnet synchronous machine(PMSM) is following:

$$P_{abc} = v_{as}i_{as} + v_{bs}i_{bs} + v_{cs}i_{cs} \quad (3.9)$$

so the dq0 reference frame power expression can be derived, as shown in formula 3.10, so the active power can be derived by the formula 3.11. The active power is the power that transformed to mechanical power in the machine mode or from mechanical to electrical in the generator mode. The back EMF e_d and e_q of the machine in dq0 reference frame can be derived by the equations 3.12 and 3.13, in the given expressions λ_d and λ_q are the $dq0$ flux linkages.

$$P_{dq0} = \frac{3}{2} (v_{ds}i_{ds} + v_{qs}i_{qs}) \quad (3.10)$$

$$P_{em} = \frac{3}{2} (e_d i_{ds} + e_q i_{qs}) \quad (3.11)$$

$$e_d = -\omega_e L_q i_{qs} = -\omega_e \lambda_q \quad (3.12)$$

$$e_q = \omega_e L_d i_{ds} + \omega_e \lambda_r = \omega_e \lambda_d \quad (3.13)$$

Using equations 3.12 and 3.13 in the expression 3.11 the active power of the machine can be derived as follows

$$P_{em} = \frac{3}{2} \omega_e (\lambda_d i_{qs} - \lambda_q i_{ds}) \quad (3.14)$$

The electromagnetic torque of PMSM can be derived in two different ways as expressed in equations 3.15 and 3.16 .

$$T_e = \frac{P_{em}}{\omega_e / \frac{p}{2}} = \frac{3}{2} \left(\frac{p}{2} \right) (\lambda_d i_{qs} - \lambda_q i_{ds}) \quad (3.15)$$

$$T_e = \frac{3}{2} \left(\frac{p}{2} \right) (\lambda_r i_{qs} + (L_d - L_q) i_{qs} i_{ds}) \quad (3.16)$$

where, p number of poles in the machine. Using following equations the control algorithm for PMSM can be developed.

The Modular Multilevel Converters

4.1 Introduction

The Modular Multilevel Converter (MMC) history starts at the year 2003, when A. Lesnicar and R. Marquardt first described the new topology in their article [23]. The first commercial use of MMC is Trans Bay Cable project in San Francisco, USA[24]. The design of MMC was provoked by the development of power generation, that required converters with multiple voltage levels. Lesnicar and Marquardt define several advantages of their innovation that have to be mentioned:

- MMC can be scaled to different voltage levels and can have various number of voltage steps;
- MMC has low total harmonic distortion;
- High availability and redundant operation;
- Failure safe operation in case of fault;
- Use of already existing standard components [23].

The main advantage of the MMC is the ability to achieve a very high voltage ratings with very clear harmonic performance. This is achieved by combining identical submodules together, each submodule is composed of simple power electronic components with low voltage rating. Use of these components allows to adapt MMC to different voltage ratings. General view of one leg of 3phase modular-multilevel converter is shown on Figure 4.1. Each converter leg consists of upper and lower arm with the n number of sub modules in each arm. The number of levels of the MMC is defined as $n+1$, where n will be the number of submodules in each arm, so the converter with 10 submodules per arm (which results in 60 submodules in the 3phase converter) will be called 11-level MMC.

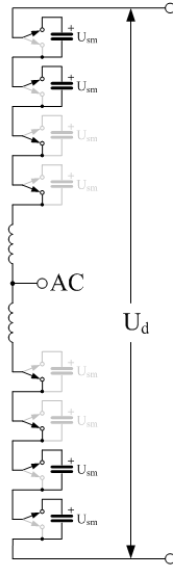


Figure 4.1: One leg of 3phase MMC [?].

Each submodule can be considered as a controlled voltage source [23]. The submodules can have 2 different types of structure: half-bridge structure Figure 4.2a a or full-bridge structure Figure 4.2b. The full bridge construction of submodules has twice the number of submodule components, which results in higher losses. At the same time the FB structure is able to suppress DC faults by blocking the IGBTs [25] [26]. For the current application the submodule half-bridge structure was used. And a further analysis will explain in detail the work of the MMC submodules.

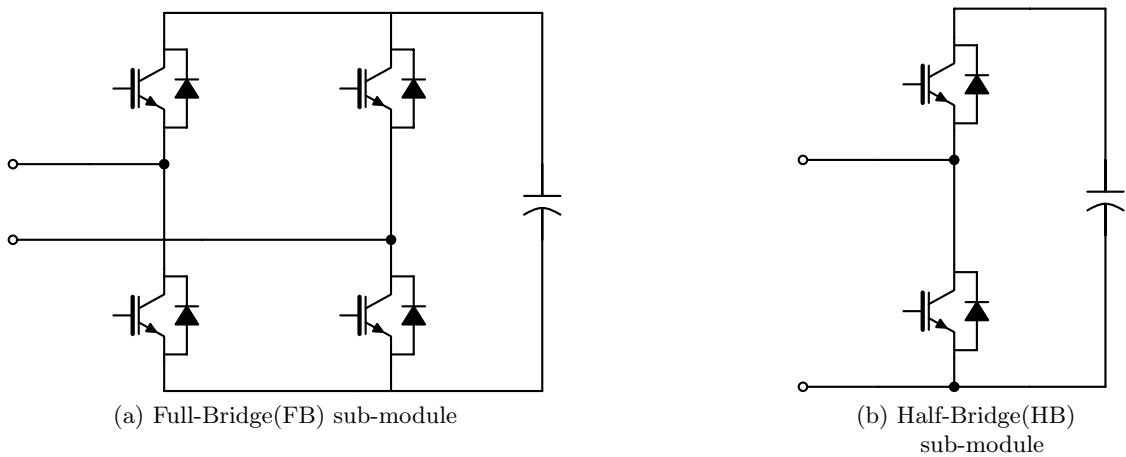


Figure 4.2: Two types of submodule configuration.

4.2 Sub-module operation principles

The submodule can be explained as a controlled voltage source, the voltage at each submodule can be switched to equal to 0 V or to capacitor voltage V_c . By switching *ON* and *OFF* different number of submodules the arm voltage can be controlled to be equal to $\frac{V_d}{2}$ [23]. There are 3 possible states of submodules: active state, bypassed state and blocked state. Active state is when IGBT $g1$ Figure 4.3 is switched *ON* and IGBT $g2$ is switched *OFF*. During Active state sub-module can have two different electrical paths, depending on the sign of the current entering the system. When $i_{sm} > 0$, so is referred as positive, the capacitor is charging through the diode $D1$ as illustrated on the Figure 4.3a. During the time when $i_{sm} < 0$, the current is flowing in negative direction and the capacitor is discharging through IGBT $g1$ as shown on the Figure 4.3b [3].

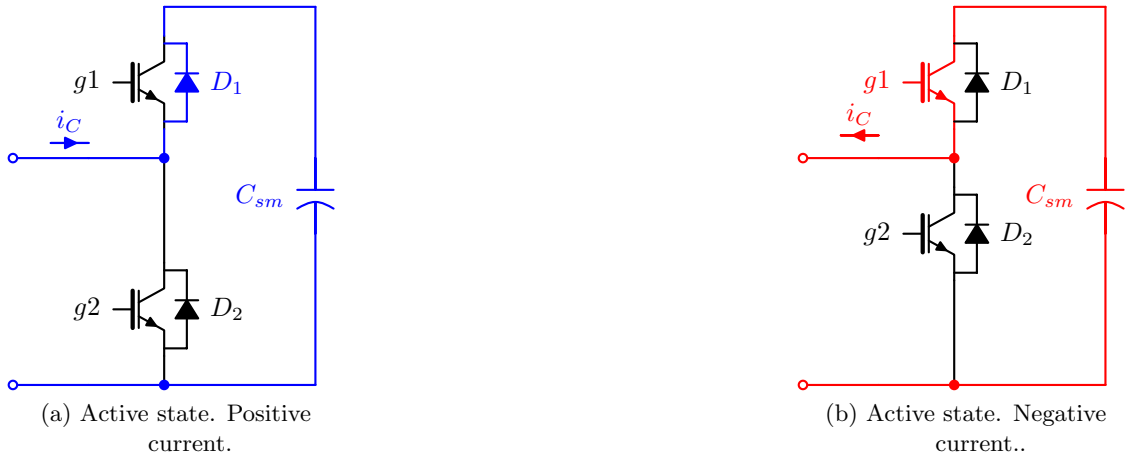


Figure 4.3: Active states of submodule operation. Where blue is for current flowing in positive direction and red is for current flowing in negative direction.

Bypassed State is characterized by the IGBT $g2$ being switched *ON* and IGBT $g1$ switched *OFF*. Similar to the active state the electric current can flow in different directions. When current flows positive direction it will pass the IGBT $g2$ as in Figure 4.4a, when the current flows in negative direction it goes through the diode $D2$ as in Figure 4.4b. This state is called bypassed, because in both modes the capacitor voltage will be equal to zero and capacitor will neither charge or discharge because it will be isolated from the rest of the system.

Blocked state is when both IGBTs $g1$ and $g2$ are turned off, so the circuit looks like the circuit depicted on the Figure 4.5. From the figure it is clearly seen that sub-module capacitor can not be discharged and it can only be charged when current is positive in active state, because only diodes $D1$ and $D2$ are conducting [3].

The equivalent circuit for normal submodule operation is present on a Figure ??, the switches $S1$ and $S2$ are the representation of IGBTs and diodes of sub-module. So the output voltage of the submodule can be defined using equation 4.1.

$$v_{c(i)} = n_{(i)} u_{c(i)} \quad (4.1)$$



Figure 4.4: Bypassed states of submodule operation. Where blue is for current flowing in the right direction and red is for current flowing in opposite direction.

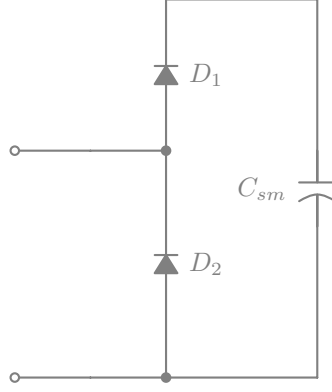


Figure 4.5: Blocked state. Both IGBT's are open.

Where u_c is the capacitor voltage; n is an insertion index and i is the number of sub-module. The insertion index n can have only two values $n=1$ or $n=0$, then the insertion index is equal to 1 that means that switch $S1$ is turned *ON* and switch $S2$ is *OFF* so the output voltage is equal to the capacitor voltage $v_c = u_c$. In case, when $n=0$, switch $S2$ is *ON* and switch $S1$ is *OFF*, so the resulting output voltage $v_c = 0$. The voltage dynamics in the sub-module capacitor can be calculated using equation 4.2.

$$C \frac{d}{dt} v_{c(i)} = n_{(i)} * i_{sm} \quad (4.2)$$

The submodule current i_{sm} is equal to the arm current (either lower arm or upper arm), because sub-modules in an arm are connected in series.

4.2.1 Balancing Algorithm

It is essential to keep equal stress distribution over the power device, for this reason submodule capacitors should operate at approximately equal voltage level [23]. The balancing algorithm is a sorting algorithm which controls converter voltage dynamics, by

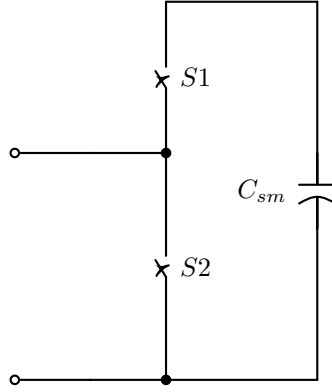


Figure 4.6: Equivalent circuit for normal operation using Ideal Switching devices.

checking the submodule voltages at every iteration and using specific sorting algorithm decides how many submodules should be switched *ON* depending on their capacitor voltage rating. To calculate the number of sub-modules that have to be inserted at each iteration, equation 4.3 is used. When controlling number of sub-modules to be inserted the capacitor voltages at each arm should have as identical waveforms as possible [3].

$$n_{arm} = \sum_{N}^{i=1} n_{(i)} \quad (4.3)$$

4.2.2 Operation of the MMC converter

where N is the number of submodules per arm.

For the successful operation of the MMC the voltage in each sub-module capacitor should be controlled to be around V_{dc}/N , where N is the number of sub-modules in one arm. This way each arm of the converter should be able to supply full dc link voltage. At the same time the sum of voltages in all the cell capacitors in the conducting path should be equal to the dc link voltage. That requirement should be fulfilled at any instant of time to eliminate the increase of the current flowing through the switches.

In the best case scenario each arm would carry half of the AC-side output current [27]. Using the Kirchhoffs current law the equations for determining the AC side current can be derived by the formula 4.4.

$$i_v = i_u(t) - i_l(t) \quad (4.4)$$

To determine the current running in the arms expressions 4.5 and 4.6 are used.

$$i_u = i_c + \frac{i_v}{2} \quad (4.5)$$

$$i_l = i_c - \frac{i_v}{2} \quad (4.6)$$

Where i_u and i_l are upper and lower arm currents respectively; i_c is the circulating current. The circulating current is the mean value of the upper and lower arm currents.

$$i_c(t) = \frac{i_u(t) + i_l(t)}{2} \quad (4.7)$$

The voltage change of the individual capacitor cells can be also derived from the arm current. For the upper arm capacitor this dynamics is described by equation 4.8, in the following expression N is the number of of the submodules, the expression for the lower arm capacitor voltages can be derived in the similar way with equation 4.9 [3].

$$C \frac{d}{dt} u_{cu}(N) = n_u(N) i_u \quad (4.8)$$

$$C \frac{d}{dt} u_{cl}(N) = n_l(N) i_l \quad (4.9)$$

where u_{cu} and u_{cl} are multi-valve voltages in upper and lower arms respectively. Similarly to the expressions 4.8 and 4.9 output voltages of individual submodule capacitors can be derived by the equation 4.10 for upper, and 4.11 for lower arms.

$$v_{cu}(i) = n_u(i) u_{cu}(i) \quad (4.10)$$

$$v_{cl}(i) = n_l(i) u_{cl}(i) \quad (4.11)$$

The output voltage of an arm of the MMC can be defined as a sum of output voltages of each capacitor in the arm as shown in equations 4.12 and 4.13.

$$v_{cu} = \sum_{i=1}^N n_u(i) u_{cu}(i) \quad (4.12)$$

$$v_{cl} = \sum_{i=1}^N n_l(i) u_{cl}(i) \quad (4.13)$$

Together with the advantages in safety, stability and availability, some complexity in operation of the converter is seen. The additional degree of freedom that converter is offering requires more complicated control algorithm. Each capacitor in the sub-module should be controlled independently and voltage levels should be compared with reference values at every operational step. Of course, there are several simplifications that can be used for easier and faster simulation, but in the real time operation the algorithm can be fairly complicated and slow. In more simple words the additional degree of freedom can be explain as follows: in common 1 level converter there is only one output AC current that can be controlled. For the MMC except of the AC current it is also required to control another current component an internal current in the converter. An internal current is the current that is flowing between lower and upper arms in one leg of the MMC. A detailed derivation of the main equations is required for the MMC. But together with the additional degree of current control of the MMC, for the converter at the grid side, when applying a current control another control component is taken into account, it is generator torque control, but that will be described more detailed in next sections. For the regulation of the number of input sub-modules in each arm a special insertion index is used. The value of the insertion index can vary between 0 and 1 and can be expressed as in equation 4.14. In this way the insertion index is the ratio of the number of inserted sub-modules to the number of sub-modules per arm.

$$n_x = \frac{\sum_{i=1}^N n_x(i)}{N} \quad (4.14)$$

where x corresponds to either upper or lower arm indicator.

At the same time the voltage waveforms of the submodules within one arm are approximately the same. To achieve that result a balancing algorithm is used. In this way the sum of submodule voltages within an arm can be defined in equations 4.15 and 4.16.

$$v_{cu} = \sum_{i=1}^N n_u(i) u_{cu} = N n_u u_{cu} = n_u u_{cu}^{\Sigma} \quad (4.15)$$

$$v_{cl} = \sum_{i=1}^N n_l(i) u_{cl} = N n_l u_{cl} = n_l u_{cl}^{\Sigma} \quad (4.16)$$

To calculate the total capacitor voltage within an arm at the instant of time equations 4.17 and 4.18 can be used for upper and lower arms respectively.

$$C \frac{d}{dt} \sum_{i=1}^N (u_{cu}(i)) = \sum_{i=1}^N n_u(i) i_u \quad (4.17)$$

$$C \frac{d}{dt} \sum_{i=1}^N (u_{cl}(i)) = \sum_{i=1}^N n_l(i) i_l \quad (4.18)$$

By inserting expressions 4.15 and 4.16 into expressions 4.17 and 4.18 respectively, equations 4.19 and 4.20 are obtained.

$$\frac{C}{N} \frac{d}{dt} u_{cu}^{\Sigma} = n_u i_u \quad (4.19)$$

$$\frac{C}{N} \frac{d}{dt} u_{cl}^{\Sigma} = n_l i_l \quad (4.20)$$

Total capacitance in the arm C_{arm} can be defined as series connection of all the capacitors within an arm 4.21.

$$C_{arm} = \frac{C}{N} \quad (4.21)$$

In case of ideal balancing algorithm capacitor voltages can be assumed to be identical, using this assumption energy stored in lower and upper arms are derived with expressions 4.22 for upper and 4.23 for lower arms.

$$w_{cu}(t) = \frac{1}{2} \frac{C}{N} (u_{cu}^{\Sigma}(t))^2 \quad (4.22)$$

$$w_{cl}(t) = \frac{1}{2} \frac{C}{N} (u_{cl}^{\Sigma}(t))^2 \quad (4.23)$$

For design of the control of the MMC it is very important to define energy unbalance and energy sum for each phase leg of the MMC. Energy sum and energy difference between lower and upper arm inputs if calculated using equations 4.24 and 4.25.

$$w_{\Sigma.c}(t) = w_{cu}(t) + w_{cl}(t) \quad (4.24)$$

$$w_{\Delta.c}(t) = w_{cu}(t) - w_{cl}(t) \quad (4.25)$$

To get closely into description of MMC control, we have to derive main voltage equations of the MMC using Kirchhoffs voltage law. Equations for the upper 4.26 and lower 4.27 arms are derived as shown further.

$$-\frac{v_{dc}}{2} + v_{cu} + L\frac{d}{dt}i_u + Ri_u + v_{mmc.out} = 0 \quad (4.26)$$

$$-\frac{v_{dc}}{2} + v_{cl} + L\frac{d}{dt}i_l + Ri_l - v_{mmc.out} = 0 \quad (4.27)$$

To determine internal MMC voltage driving circulating current equations 4.26 and 4.27 have to be added. By adding these two equations expression for circulating current is obtained 4.28

$$-v_{dc} + v_{cu} + v_{cl} + R(i_u + i_l) + L\frac{d}{dt}(i_u + i_l) = 0 \quad (4.28)$$

Equation 4.28 can be also expressed as a function of circulating current. That will give u_c which is internal voltage in the MMC driving circulating current.

$$u_c(t) = Ri_c(t) + L\frac{d}{dt}i_c(t) \quad (4.29)$$

Similarly the internal voltage of the MMC that is driving grid current can be derived by difference between equations 4.26 and 4.27.

$$v_{cu} - v_{cl} + R(i_u - i_l) + L\frac{d}{dt}(i_u - i_l) + 2v_{mmc.out} = 0 \quad (4.30)$$

$$e_v(t) = \frac{R}{2}i_v(t) + \frac{L}{2}\frac{d}{dt}i_v(t) + v_{mmc.out} \quad (4.31)$$

where e_v is the internal MMC voltage that drives the grid current. Important observation is that both circulating i_c and the grid i_v currents are driven by MMC voltages u_c and e_v . At the same time these voltages depend on the sum (difference) of voltages from both upper and lower multivalves as expressed in equations 4.32 and 4.33.

$$u_c(t) = \frac{v_{dc}}{2} - \left(\frac{v_{cu}(t) + v_{cl}(t)}{2} \right) \quad (4.32)$$

$$e_v(t) = \frac{u_{cu}(t) - u_{cl}(t)}{2} \quad (4.33)$$

It is also important to control energy change in the MMC. Energy dynamic change in one arm is defined as product of arm current and output voltage from arm submodules, equation 4.34 represents energy dynamics in the upper arm and equation 4.35 in the lower arm [3].

$$p_u(t) = v_{cu}(t)i_u(t) \quad (4.34)$$

$$p_l(t) = v_{cl}(t)i_l(t) \quad (4.35)$$

Similarly the sum and difference between upper and lower arm energy inputs can be derived like in equations 4.36 and 4.37 respectively.

$$p_{sum}(t) = v_{cu}(t)i_u(t) + v_{cl}(t)i_l(t) \quad (4.36)$$

$$p_{dif}(t) = v_{cu}(t)i_u(t) - v_{cl}(t)i_l(t) \quad (4.37)$$

Following expressions can be also written after insertion of circulating and grid currents and multivalve voltages to represent energy dynamics of the MMC.

$$p_{sum}(t) = w_{\Sigma}(t) = -e_v(t)i_v(t) + (v_{dc} - 2u_c(t))i_c(t) \quad (4.38)$$

$$p_{dif}(t) = w_{\Delta}(t) = \frac{i_v(t)}{2}(v_{dc} - 2u_c(t)) - 2e_v(t)i_c(t) \quad (4.39)$$

4.2.3 Mathematical modeling of MMC

There are two possible way to obtain MMC mathematical model:

- State equations model
- Energy equations model [3].

In the following design Energy equations model was used. Energy representation model consists of two different components one for circulating currents and another one for the energy stored in the capacitors in each arm. In this model insertion indexes are not taken into account and control is performed directly by driving voltage of the circulating current u_c and driving voltage of the grid current e_v . The internal behavior of this two components is non-linear, so in the reference Phd thesis [3] was proposed simplified system for their definition.

Circulating current i_{ck} and grid current i_{vk} can be represented in matrix form as in matrix 4.40.

$$\frac{d}{dt} \begin{bmatrix} i_{ck} \\ i_{vk} \end{bmatrix} = \begin{bmatrix} -\frac{R}{L} & 0 \\ 0 & -\frac{R'}{L'} \end{bmatrix} \begin{bmatrix} i_{ck} \\ i_{vk} \end{bmatrix} + \begin{bmatrix} \frac{u_c}{L} \\ \frac{e_v - v_{pcc}}{L'} \end{bmatrix} \quad (4.40)$$

On basis of the previous assumptions it can be stated that the grid system is linear and can be controlled independently from the inner system of the converter and fluctuations in the capacitive energy dynamics do not influence outer loop.

The energy stored in the capacitors is controlled independently, using the matrix 4.41, where $w_{\Sigma k}$ is energy sum and $w_{\Delta k}$ is energy difference of energy stored in capacitor arms.

$$\frac{d}{dt} \begin{bmatrix} w_{\Sigma k} \\ w_{\Delta k} \end{bmatrix} = \begin{bmatrix} v_{dc} - 2v_{ck} & -e_{vk} \\ -2e_{vk} & \frac{1}{2}(v_{dc} - 2u_{ck}) \end{bmatrix} \begin{bmatrix} i_{ck} \\ i_{vk} \end{bmatrix} \quad (4.41)$$

The regulation of the capacitive energy stored in submodules can be achieved by controlling circulating and grid currents of the MMC. At the same time currents can be controlled independently from energies and in this way control will be subdivided into the outer loop, for controlling energy at every iteration, and inner loop to control circulating current dynamics.

4.3 Determination of parameters of the semiconductor devices

The selection of semiconductor components suitable for a specific converter is one of the key figures in the converter control and reliable operation. As mentioned earlier the sum of the capacitor voltages in one arm should be approximately equal to the DC side rms voltage. So ideally each capacitor should be controlled to be at the same voltage level, according to the expression 4.42. When selecting the size of sub-module capacitance, the formula 4.43 can be used.

$$U_{SM} = \frac{U_{DC}}{N} \quad (4.42)$$

where U_{DC} is DC link voltage and N is a number of submodules in arm.

$$C_{SM} = \frac{\Delta W_{SM}}{2\epsilon U_{SM}^2} \quad (4.43)$$

where ΔW_{SM} is the sub-module energy change and it can be calculated as follows

$$\Delta W_{SM} = \frac{2}{3} \cdot \frac{S}{k \cdot \omega_n \cdot N} \cdot \left(1 - \left(\frac{k \cdot \cos\phi}{2}\right)^2\right)^{\frac{3}{2}} \quad (4.44)$$

where S is the converter apparent power, k is voltage modulation index, ω_n is the output angular frequency and $\cos\phi$ is the power factor (PF) [2].

In each arm of the MMC one inductor is added for limitation of current harmonics and fault currents [28]. For the sustainable design of the arm inductance several aspects have to be taken into account:

- Resonance with the cumulative arm capacitance C_{arm} ;
- Current derivative of each arm in case of DC faults [29].

Using Kirchhoff's voltage law, arm inductance $L_{arm.res}$ resonant to the capacitance C_{arm} can be determined as in equation 4.45 [29].

$$L_{arm.res} = \frac{1}{C_{arm}\omega^2} \frac{2(h^2 - 1) + m_a^2 h^2}{8h^2(h^2 - 1)} \quad (4.45)$$

where h is the harmonic level; ω is the converter operating frequency $\omega = 2\pi f$, for $f=50$ Hz; and m_a is the modulation index [29] [30].

Very important is to avoid resonances at even harmonics, especially of a low order, like second and fourth. The arm inductance is usually selected depending on the value of cumulative arm capacitance, in such a way that second order harmonic is eliminated. Using Figure 16.11 from the book "High Voltage Direct Current Transmission: Converters, Systems and DC Grids" [29] it can be stated that arm inductance usually lies in the range 30-100 mH.

The maximum value of arm inductor is derived considering current derivative during DC faults is calculated with the formula 4.46.

$$L_{arm_max} = \frac{U_{DC}}{(dI_{DC}/dt)_{critical}} \quad (4.46)$$

The critical current for the semiconductor devices like IGBT's and diodes lies in range $100 - 1000 A/\mu s$. Inserting critical current value into the formula 4.46 we obtain value below mH , in this way maximum inductor value is lying in more broad range then resonance inductor parameter. In practice value of arm inductor should be used in range of 0.5-0.15 pu from the converter rating [29].

Control of the wind turbine

5.1 Review of the system structure

After literature review on the MMC implementation in Wind power technologies, it is possible to conclude that quite significant amount of research was done on using modular multilevel converter for the grid side connection of the wind turbine. In the following research I tried to use two back to back MMC converters both from the grid side and the machine side. Considering different kinds of MMC advantages, it would be interesting to see how much system will gain can gain in terms of efficiency, safety and operation of the wind turbine, when MMC converter is used also on the generator side.

The block scheme of the back to back MMC converter is presented on the Figure 5.1. The big question when designing this structure is sustainable system control. MMC op-

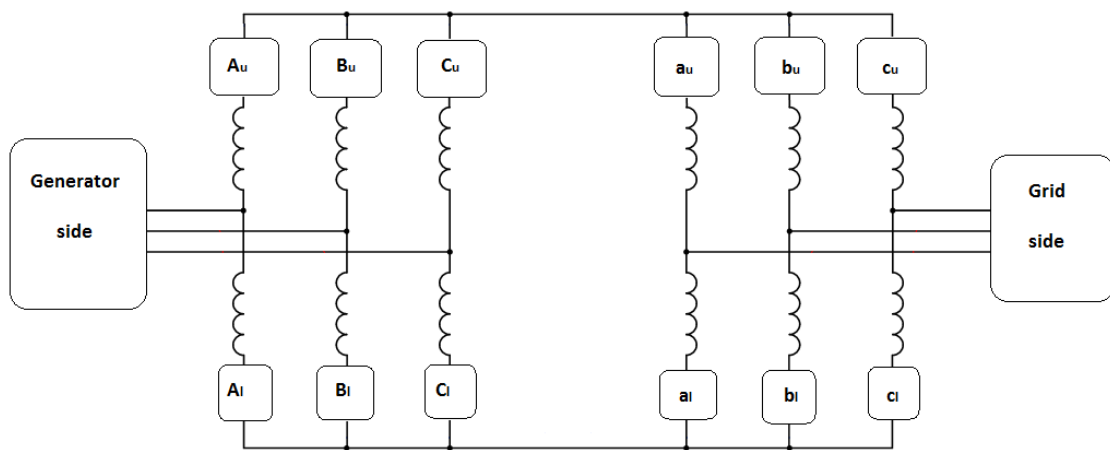


Figure 5.1: Schematic representation of back-to-back MMC for the Wind turbine.

eration requires control of 2 main current components: ac output current and circulating

current in the converter. Control of the grid side MMC is well described in the literature. However, wind turbine generator requires the speed control, to maintain generator torque to keep constant power supply. In this way control of the generator side MMC is more complicated, it has to take into account, ac side current, circulating current and generator rotational speed. All three aspects will be described in detail in next paragraphs.

5.2 Control of permanent magnet synchronous generator

5.2.1 Modeling of drive train

The drive train is responsible for the torque at the rotor to the generator torque. Drive train modeling for the studies of wind turbine system can be reduced to simple kinematic conversion using transfer function. [31] The transfer function is shown in 5.1

$$G(s) = \frac{K\omega_n^2}{s^2 + 2\zeta\omega_n s + \omega_n^2} \quad (5.1)$$

where, ζ is the damping ratio, ω_n is the natural frequency, and K is the gain for the drive train, in case of Direct Drive topology $K=1$, because there is no gear-box. With the help of transfer function it is possible to define parameters of the torque and speed control in 5.2 5.3 correspondingly. [31]

$$T_{em} = G(s)T_{wt} \quad (5.2)$$

$$\omega_m = k_{gear}\omega_{wt} \quad (5.3)$$

where T_{em} is the electromagnetic torque and ω_m is mechanical speed of the system.

5.2.2 Modeling of PMSG

To describe the generator control, system parameters will be transferred to $dq0$ reference frame. The control model of PMSG consists of two voltage equations 5.4 5.5 and one torque equation 5.6.

$$u_d = R_s i_d + L_d \frac{di_d}{dt} - \omega_e L_q i_q \quad (5.4)$$

$$u_q = R_s i_q + L_q \frac{di_q}{dt} + \omega_e \psi_{PM} + \omega_e L_d i_d \quad (5.5)$$

$$T_{em} = \frac{3}{2} n_{pp} (\psi_{PM} i_q + (L_d - L_q) i_d i_q) \quad (5.6)$$

where u_d and u_q are voltages in $dq0$ reference frame; i_d and i_q are currents in $dq0$ reference frame; R_s is the stator resistance; L_d and L_q are the inductances in $dq0$; ω_e is the electrical rotating speed; ψ_{PM} is the flux linkage established by permanent magnets and n_{pp} is the number of pole pairs in the generator. The rotational speed of the generator can be defined as 5.7.

$$\omega_e = n_{pp}\omega_m \quad (5.7)$$

To simplify modeling inductance's L_d and L_q can be assumed equal $L_d = L_q$. In this case mechanical torque can be rewritten as 5.8.

$$T_{em} = \frac{3}{2} n_{pp} \psi_{PM} i_q \quad (5.8)$$

To control the torque it is required to determine the moment of inertia $J[kg \cdot m^2]$ that is required by the system, to supply constant power. The relation between torque and inertia is defined in 5.9.

$$T_{em} - T_L = J \frac{d\omega_m}{dt} \quad (5.9)$$

where T_L is the load torque.[31]

5.3 Control of the two-level inverter

Different control strategies for simple two-level inverter in wind energy applications are present in the literature [18] [32] [33] [34] [31]. If the reader is interested in detailed description of different control strategies for PMSG interfaced with two level inverter I would suggest to take a look at references cited above.

For the simulation of two-level inverter topology, the Indirect Field-oriented Control was used. We will not focus in this thesis in the control of the grid side two-level inverter. A brief explanation of the generator side control of the two-level inverter is described below. In the Figure 5.2 algorithm of the Indirect Field-oriented Control (IFOC) of the Permanent Magnet Synchronous Generator is shown. For the correct implementation of it is necessary

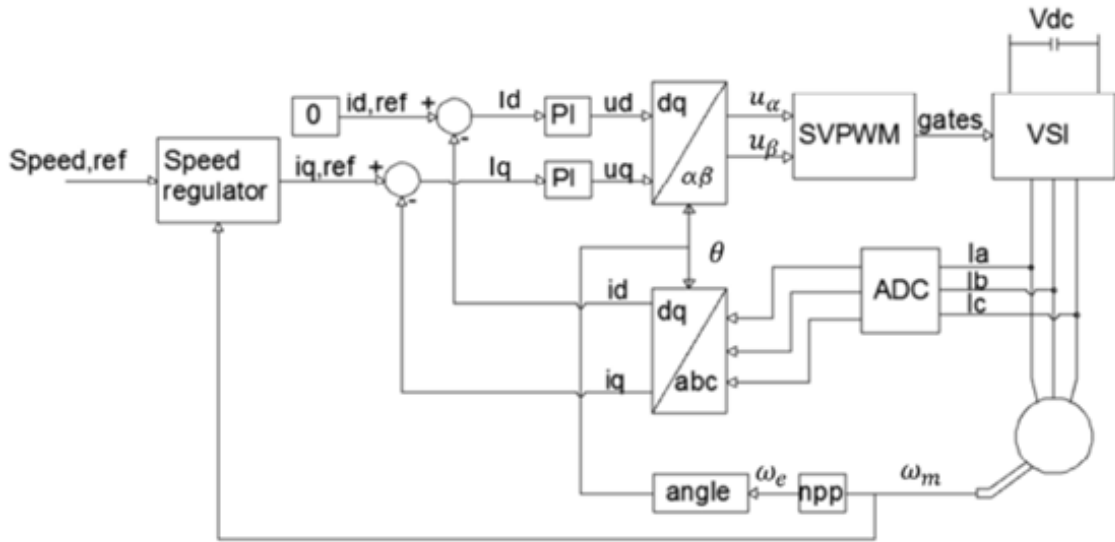


Figure 5.2: Indirect Field-oriented Control of PMSG [35].

to know the position of currents and voltages in $dq0$ axes. At first it is necessary to measure rotor position and abc currents of the stator. After measuring abc currents are transformed to $dq0$ reference frame using Park's transformation. Afterward dq currents are compared with the desired reference values and by PI proportional-integral blocks are

transformed to desired d and q voltage responses. At the end dq voltages are transformed back to abc reference frame and used as an input to Space-Vector Modulation block, where pulses for the converter gates are created.

5.4 Control of the MMC

Both equations 4.26 and 4.27 are valid for the grid and for the machine side converter. We assume ideal converter operation, so the voltage drop across the inductor is not taken into account. On this basis equations for the MMC voltage are obtained.

$$v_{mmc} \approx \frac{v_{dc}}{2} - v_{cu} \approx \hat{v}_{mmc} \sin(\omega t + \phi) \quad (5.10)$$

$$v_{mmc} - \frac{v_{dc}}{2} + v_{cl} \approx \hat{v}_{mmc} \sin(\omega t + \phi) \quad (5.11)$$

The AC side of the MMC is operated at the same frequency as system frequency. The ac side signal is controlled to have sinusoidal characteristic, to achieve that there are several main requirements for the MMC operation. Upper and lower multivalve voltages should be controlled to be around half value of v_{dc} and the resulting 3phase mmc voltage will be an offset-free value. Both of the fundamental components should be around \hat{v}_{mmc} . If we take a detailed look into upper and lower multivalve voltage control they should be controlled to be in counter phase to each other, and at the same time the lower component should be in phase with the output (input for generator side) MMC 3phase voltage. In this way the resulting output voltage is close to v_{dc} value. Considering previous requirements we can specify the value for the individual capacitor values in each of submodules. The voltage through the capacitor is determined by $\frac{v_{dc}}{N}$, where N is the number of submodules in each of the arms.

5.4.1 Different modulation techniques for MMC

There are several different modulation techniques used for creating MMC input signals. The modulation strategy is important in order to achieve high-quality waveforms of the converter output signals.

Nowadays very popular and simple modulation technique that is used is conventional pulse-width modulation. The main working principle behind it is the use of two signals, one is a reference waveform and another one is the carrier signal. The carrier signal can be of three different forms: the saw-tooth or triangular shaped waveforms. The reference signal is compared with the carrier, if the reference signal is higher, then the output pulse will be high, otherwise it will be low. In the half-bridge circuit such a PWM pulse will control the upper IGBT and the inverse of that pulse will control the lower IGBT in the circuit. The MMC generally consists of several half bridge modules in each arm, so to simulate PWM signal the number of carriers used should correspond to the number of submodules. The carrier modulation of the MMC can be done in a several different way, the carrier signals can be shifter in phase for example (phase/shifted modulation), so each $N+1$ carrier has a phase shift delay before it reaches the reference signal. The other way is to have number of pulses that have different levels (level-shifted modulation). Both

phase and level-shifted modulation techniques are shown on the Figure ???. Level-shifted modulation can also have several different variations, but they are not under scope of current research.

When the MMC has a big number of submodules the simulation of PWM becomes complex and requires a lot of small repetitions. For the current research other signal modulation strategy was used. The Space-Vector Modulation was used to generate gate signal for the converter. The SPM techniques are based on the generation of the reference signal, the reference signal is an average of the value in range between two possible discrete output values over certain switching period [36]. Depending on the complexity of the control SVM can have, 3-D, 2-D and 1-D control regions. Using the data from [36], where different techniques were compared and evaluated, the decision was made that SVM based on 1-D control region will be used for simulations within current project.

Space-Vector modulation (SVM)

The choice of correct modulation strategy can influence to a great extent the output waveforms of the converter and also simplify or complicate the simulation procedure. The main idea behind SVM is the generation of the reference voltage vector. The reference vector is generated as an average value between possible output discrete voltages of the converter during the switching period. [36]. For calculation of the reference voltage, the converter control region should be determined. The control region is based on different switching states, For each switching period the state vectors located closer to the reference vector are determined. Depending on SVM technique, different kinds of calculations are used to determine state vectors and the times of switching. The higher the number of levels in the converter, the more complicated is to define necessary control region for each converter state [36].

Conventional SVM can have different kinds of control regions, as referring to [36] where SVM techniques based on 3-D and 2-D control regions are described. As shown in the paper, there is another SVM technique which has similar properties as conventional SVMs, but it is based on single-phase multilevel modulator and is much simpler in implementation, than the conventional SMV.

Comparison between conventional SVM techniques and single phase SVM (1DM) is presented in the paper [36]. In addition to reduced complexity of implementation 1DM SVM gives a possibility to use Space-vector modulation with multiphase converters. The calculation method which helps to determine reference voltage of 1DM converter is also described in [36]. To generate the reference voltage the system of non-linear equations should be solved for each converter phase.

During the research process I tried to apply 2 different modulation strategies one is the phase carrier modulation with the phase shifted waveforms for each sub-module and second one is the use of one dimensional space vector modulation. For the 11-level converter simulation of the phase-shifted carrier modulation can take a significant amount of time, because all the levels should have input signals to be generated separately. After studying of Space Vector Modulation techniques that are proposed in different literature the decision was made to use 1DM modulation technique, because classical way of detecting reference vector, that is proposed in [37] [38]. Hexagon models described in [37] [38] will have an extra ring for each additional converter level, in this way the simulation becomes very complex and time consuming.

Therefore one dimensional (1DM) space-vector modulation was used to achieve fairly fast simulation. This modulation is described in detail in an article [36]

Using 1DM can reduce multilevel modulation problem to two-level modulation problem. This strategy can be used for multi-phase systems; the number of phases will only influence the number of cases to be studied. In our case 3-phase system is used and for 3-phase system number of cases is equal to six. [36]

The decision about the specific applied case should be taken on basis of comparison between magnitudes of the reference vectors. The comparison gives the necessary normalized reference vector. [36]

The algorithm in the 5.3 represents the simulation sequence for three phase converter, the big advantage of the algorithm proposed in [36] is that it can be used for the converter with any number of levels. Switching sequence and switching time for the converter modulation are proposed in the 5.1.

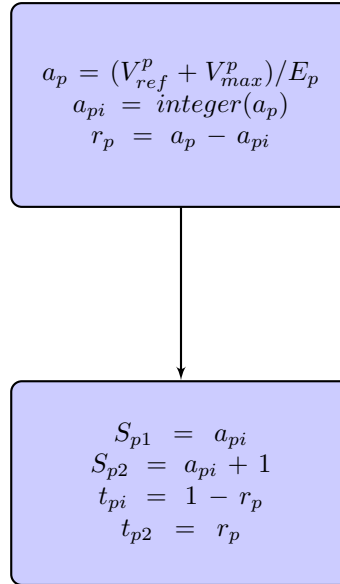


Figure 5.3: 1DM modulation algorithm for one phase of the converter.

Table 5.1: 3 Phase system equations determining switching sequence and switching times by 1DM modulation principle. [36]

Phase1	Phase2	Phase3
$S_{11} = a_{1i}$	$S_{12} = a_{2i}$	$S_{31} = a_{3i}$
$S_{12} = a_{1i} + 1$	$S_{22} = a_{2i} + 1$	$S_{32} = a_{3i} + 1$
$t_{11} = 1 - r_1$	$t_{21} = 1 - r_2$	$t_{31} = 1 - r_3$
$t_{12} = r_1$	$t_{22} = r_2$	$t_{32} = r_3$

In practice to simulate control of multilevel converter using space-vector modulation, the 3phase signal is compared with reference signal, then it's regulated by PI control. Control

signal will be modulated by 1DM vector modulation and then using balancing algorithm adjusted for each of the submodules in the phase leg.

5.4.2 Control of the MMC's outer loop energy dynamics

The mathematical model behind the MMC control was described in detail in 4. As far as MMC is of a VSC type, it's outer control will be similar to the control of any two-level VSC. The control of the outer-loop energy dynamics is adapted from the [5] where the energy sum control part is described in detail. This control loop is applied to the grid

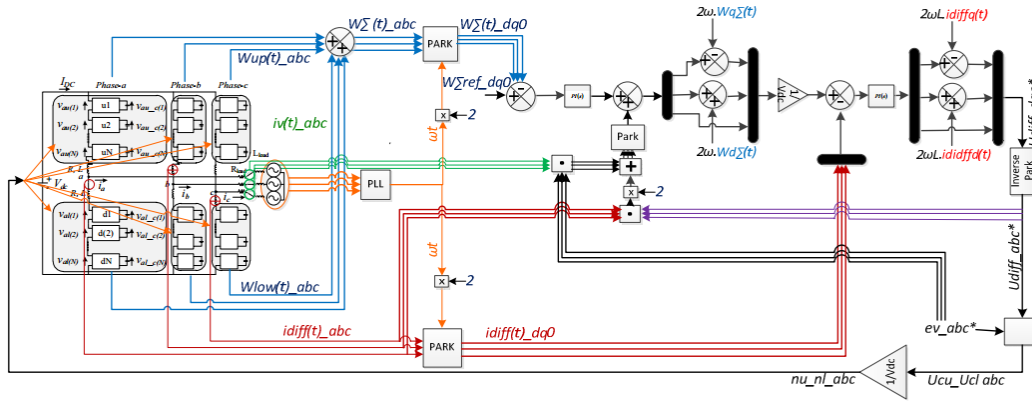


Figure 5.4: Energy sum control scheme.[5]

side MMC converter. The generator side MMC energy dynamics control will be described further.

5.4.3 Circulating current control

The circulating current of the MMC is kept constant by controlling the energy difference in the converter.

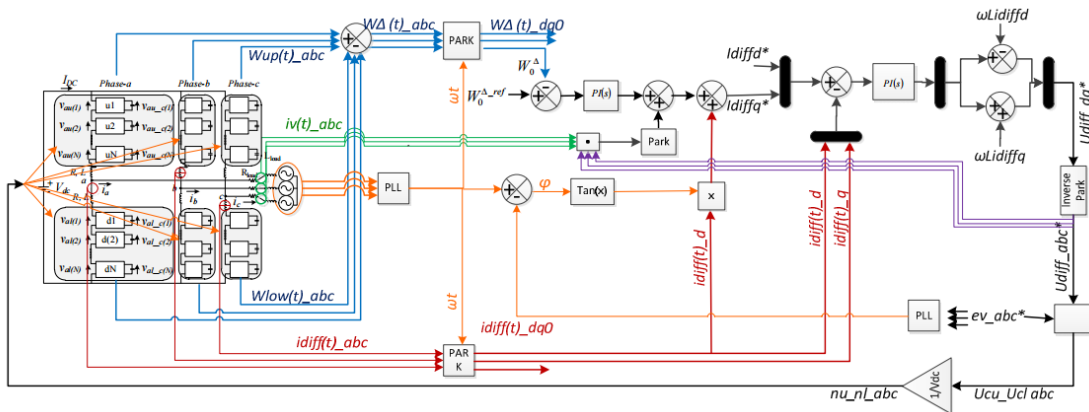


Figure 5.5: Energy difference control scheme.[5]

5.4.4 Control of the generator side MMC

One of the main challenges experienced during this thesis is combination of the MMC control scheme with the speed control required for the generator reliable operation. During the literature study very few information was found on the use of Modular Multilevel Converters for Wind Energy application and even less on the MMC that are used to control generator rotational speed or torque input. To control the generator side MMC control strategies of the grid side MMC and simple two-level voltage-source inverter were combined by the student.

The circulating current control loop is kept the same as for the grid side converter, but the energy difference control was changed, by first controlling the output generator abc currents and rotor position angle θ . This part is basically adapted from the two-level VSC. Similarly to the two-level VSC 3 phase currents are transformed to the $dq0$ reference frame; compared with the reference values using PI controllers (one for the d-axis current and one for the q-axis current) and then transferred back to the abc reference frame. That component will replace the e_v voltage that is defined in Section 4.2.2, that is driving grid side current.

Simulation and Results

6.1 General structure

General structure of the Simulation model developed by the master student is shown in the Figure 6.1. The model can be subdivided into several parts:

- Generator part 6.2
- Back-to-back MMC blocks 6.5
- Control blocks for generator side and grid side MMC's 6.9
- Blocks for control signal modulation 6.8
- Balancing algorithm implementation 6.6

Step by step implementation of the developed wind turbine system is described below.

6.2 Generator side

A part of the model that represents wind energy conversion model described in Figure 2.3 is represented as MatLab Simulink structure in the Figure 6.2. It contains the Permanent Magnet Synchronous generator and the Wind Turbine, that is generating torque input to the wind turbine.

6.2.1 Simulation of the wind turbine in MatLab Simulink

For the simulation of the wind turbine the block called "Wind Turbine" from MatLab Simulink Library was used. In the 6.3 we can see the Mask of the Simulink block Wind Turbine. It can be clearly seen from the figure, that block directly represents main wind

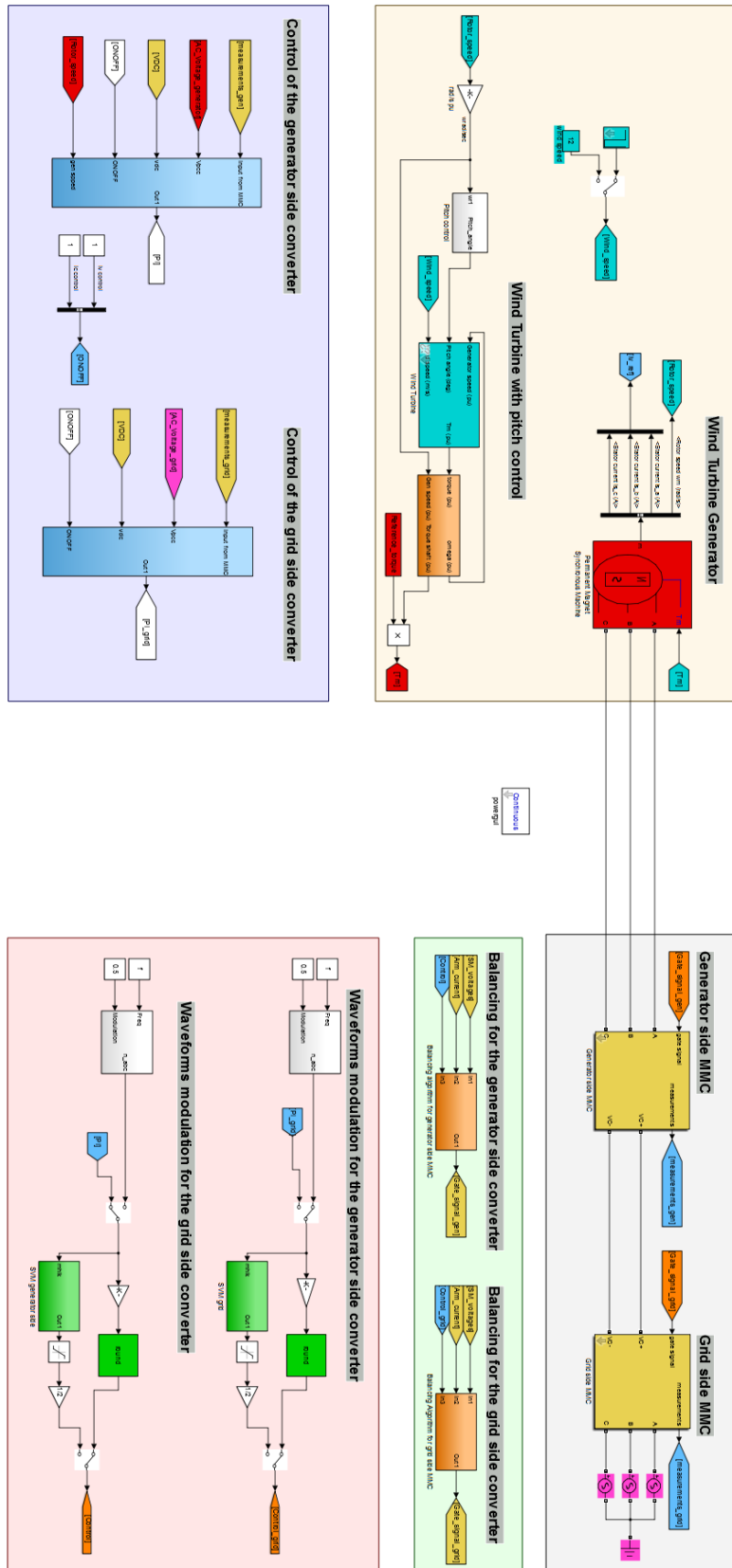


Figure 6.1: Matlab Simulink model for the simulation of the 10 MW wind turbine with back-to-back MMC converter.

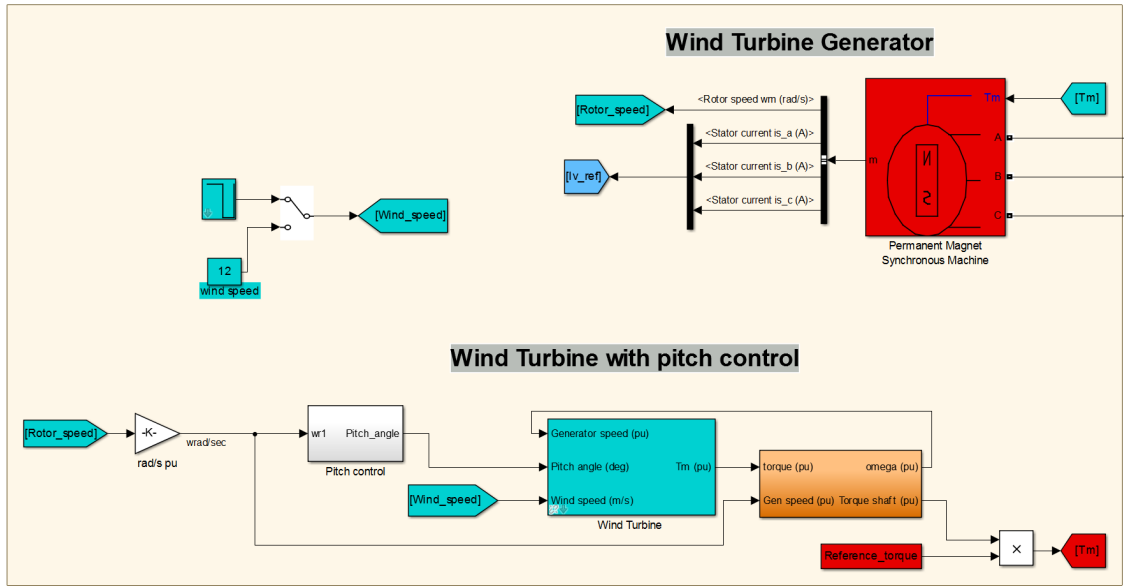


Figure 6.2: Wind Turbine and Wind Turbine Generator part of MatLab Simulink model.

conversion equations. The input parameters of the wind turbine are listed in the Table 6.1.

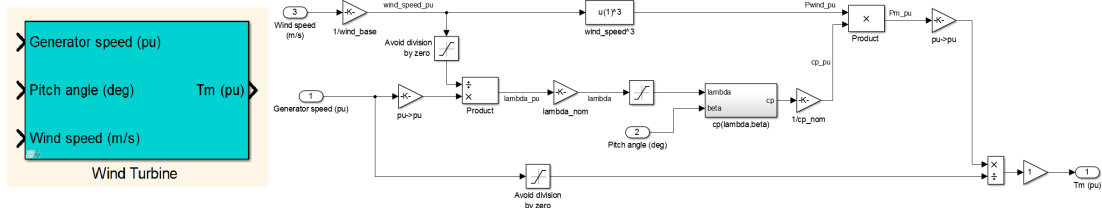


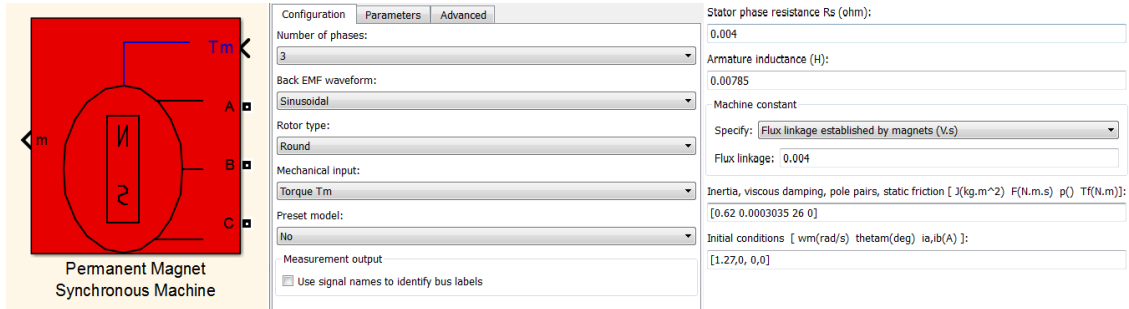
Figure 6.3: MatLab Simulink Wind turbine block and its mask structure.

6.2.2 PMSM simulation parameters estimation

For correct simulation of the wind turbine in MatLab Simulink it is important to use sufficient Generator parameters when designing the model. MatLab Simulink Library provides already built block for simulation of PMSG, that block requires several input parameters for simulation. The Simulink block and required parameters are listed in 6.4. The calculation of generator parameters was beyond the scope of this thesis, so the necessary input data was taken from several references with similar power and voltage requirements. [39] [40] [41]. Selected parameters for the generator are shown in the 6.1.

Table 6.1: Input parameters of Permanent Magnet Synchronous Generator (PMSM).

Initial parameters	
Wind Turbine parameters	
Rated power (MW)	10
Rotor speed (rpm)	12.3
Rotor diameter	154
Tip speed ratio	7,8
Generator parameters	
Rated Voltage (V)	3300
number of pole pairs	160
rated wind speed (m/s)	12
air mass density (kg/m ³)	1.225
Stator phase resistance (Ohm)	0.0366
Phase inductance (mH)	3.6
Generator efficiency %	0.99
Calculated parameters	
Power at the generator shaft (MW)	10,7
Generator moment of inertia (kg.m ²)	0.62
Torque (M Nm)	7.4

**Figure 6.4:** MatLab Simulink block parameters for Permanent Magnet Synchronous Generator (PMSG).

6.3 Simulation of the Modular Multilevel Converter

6.3.1 Parameter estimation of the Main MMC components

Using equations from the Chapter 4 input parameters for the modular multilevel converter semiconductor components were calculated. An initial function was developed to make possible to adjust simulation model depending on desired values, such as Voltage, Current, number of submodules in the MMC arm etc. The initial function is listed in the Appendix A. Calculated parameters for 11-level and 6-level MMC are listed in the Table 6.2.

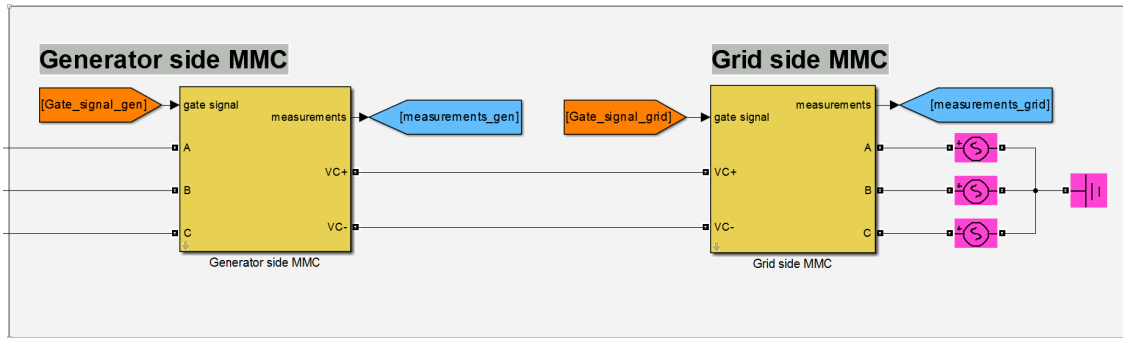
The MMC masks are mirrored to simulate back-to-back structure as shown in the Figure 6.5. For the implementation of the control it is necessary to measure several MMC parameters:

Table 6.2: MMC submodule calculated input parameters

Parameter	MMC 11-levels	MMC 6-levels
Number of SMs in arm	10	5
DC voltage, Vdc, V	5388	5388
Submodule voltage, Vsm, V	538	1077
Submodule capacitance, Csm, mF	25,6	53
Arm inductance, Larm, mH	24,8	46,5

- Arm current is measured at the ac output side of each arm using ampere-meter.
- The sum of submodule output voltages for each arm. Each submodule has its voltage measured by the voltmeter at the capacitor side, then signals are summed together.
- Separate voltages of each submodule are the necessary input to the balancing algorithm.
- And the last important measurement is arm voltage.

Using all the above-mentioned parameters the converter voltages are controlled and input gate signal is generated.

**Figure 6.5:** Generator side and grid side MMC converters

6.3.2 Balancing algorithm

The Simulink model contains 2 masks called "Balancing algorithm" shown in the Figure 6.6. Balancing algorithm is necessary to check the submodule voltage dynamics at each control iteration and take a decision to switch submodules from active to bypassed state. Appendix B contains MatLab function that is used to balance voltages in each arm. To check if the balancing algorithm is implemented correctly output voltages of two submodules from the same arm are compared as shown in the Figure 6.7. If the waveforms repeat each other completely, then it can be said the balancing algorithm was implemented correctly.

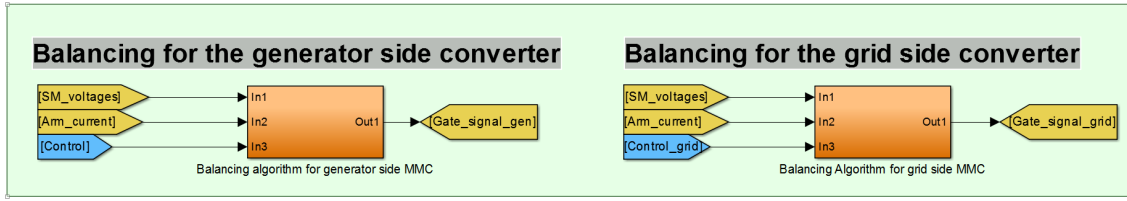


Figure 6.6: Balancing algorithm for both generator and converter side converters.

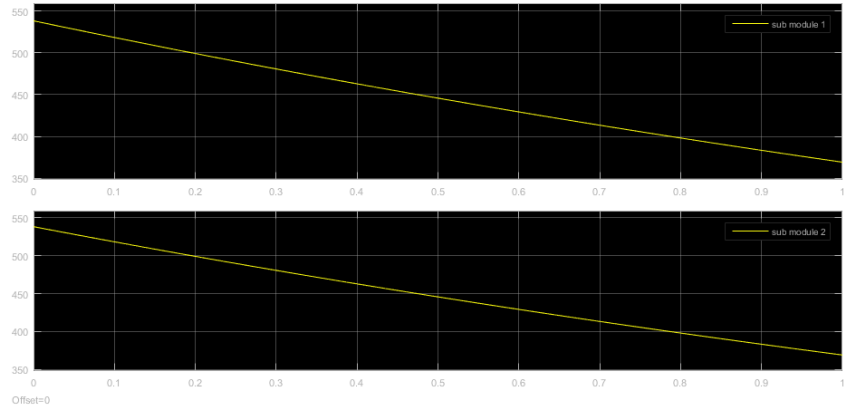


Figure 6.7: Successful implementation of balancing algorithm.

6.4 Control of output parameters

The control strategy describe in above sections is simulated with the following structures 6.8, 6.9. The signal modulation was build in two different way. The round function was used during tuning of the model, when interfacing generator with the MMC converters. The round function is faster then the block for generation of modulation signal.

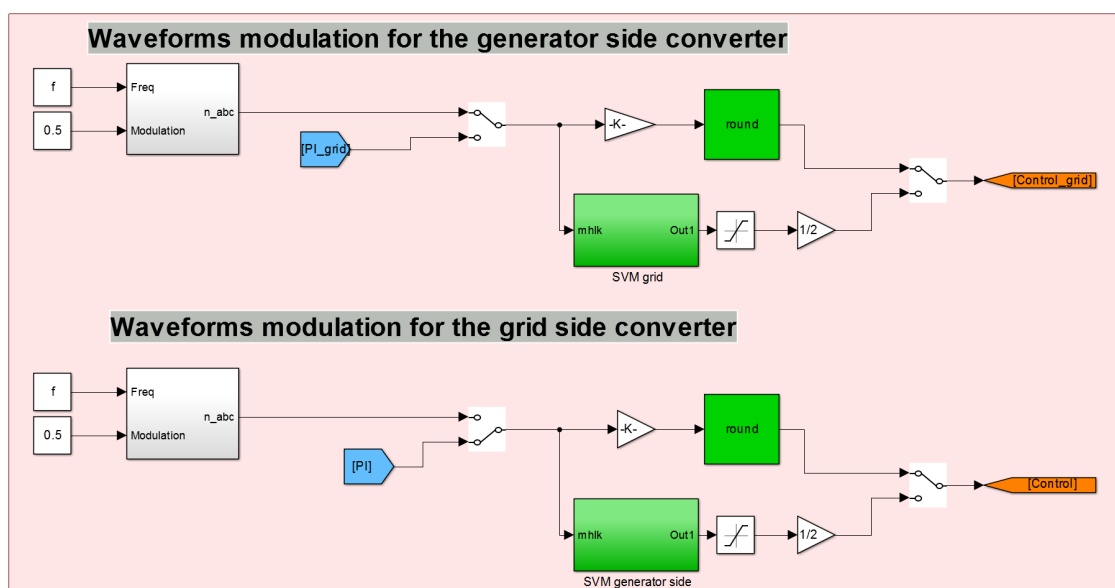


Figure 6.8: Signal modulation blocks for both MMCs

PI control loops are complex and will not be described in a very detail in this report. It have to be mentioned that PI controller for the generator side has additional input in a form of rotor position angle θ .

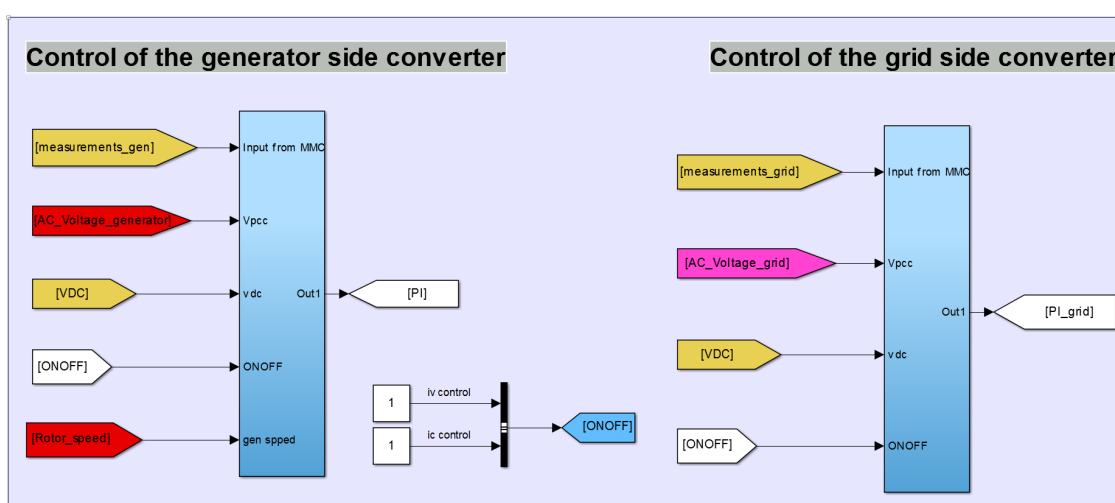


Figure 6.9: Control blocks for both generator side and grid side converters.

6.4.1 Output of the converter control

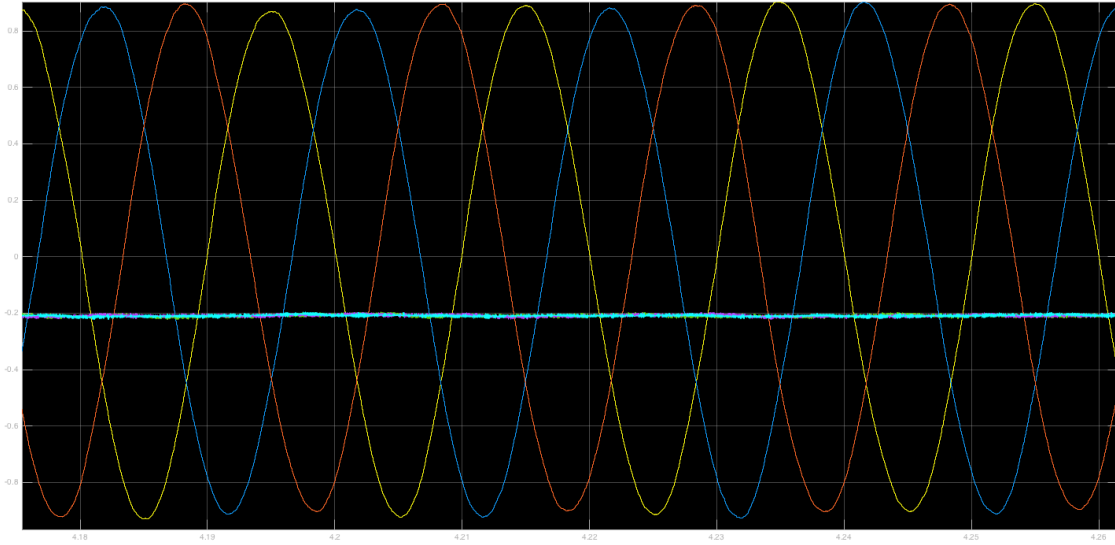


Figure 6.10: Output waveforms of the circulating and output MMC currents for the grid side converter.

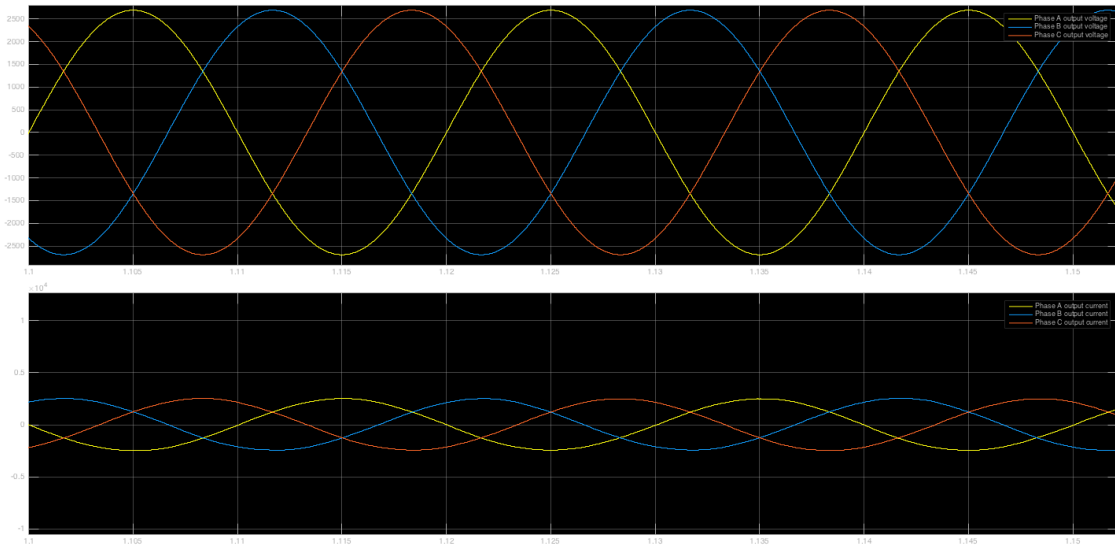


Figure 6.11: 3 phase output currents and voltages measured at the grid side.

To generate output signal for the converter voltages driving grid current and circulating current are added using sheme from the Figure ?? Control input and output voltages driving grid current are plotted in the Figures 6.15 and 6.14 Waveform of the voltage driving the circulating current of the MMC u_c is shown in the Figure 6.16. The control output of the voltage driving the circulating current of the MMC is shown in the Figure 6.17.

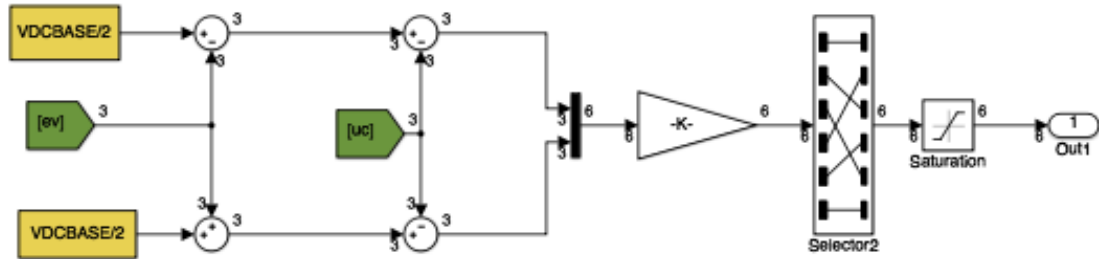


Figure 6.12: Comparison of outer loop and inner loop control outputs for converter gate signal generation. [3]

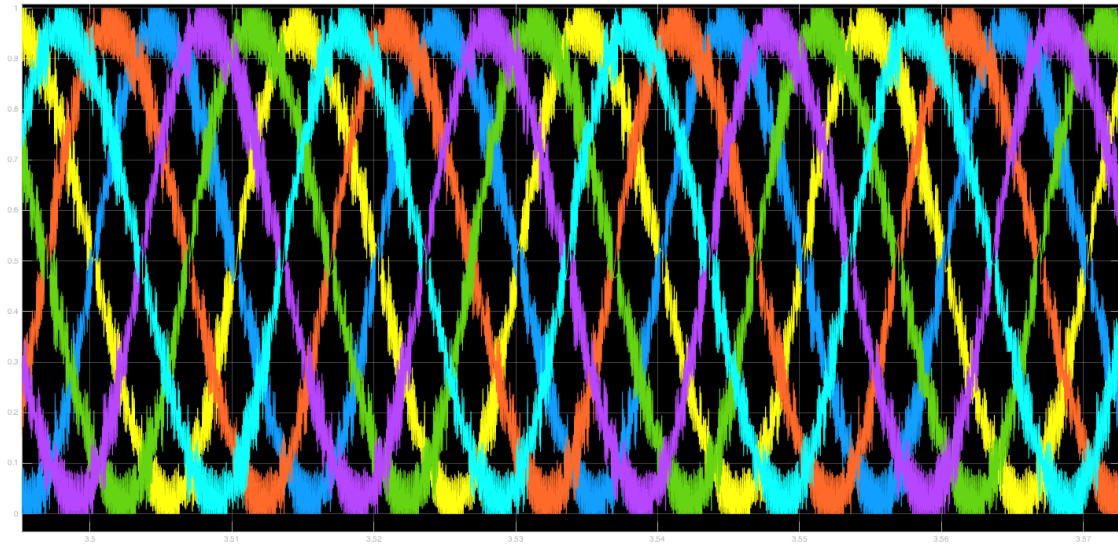


Figure 6.13: Output voltage signal from the PI converter.

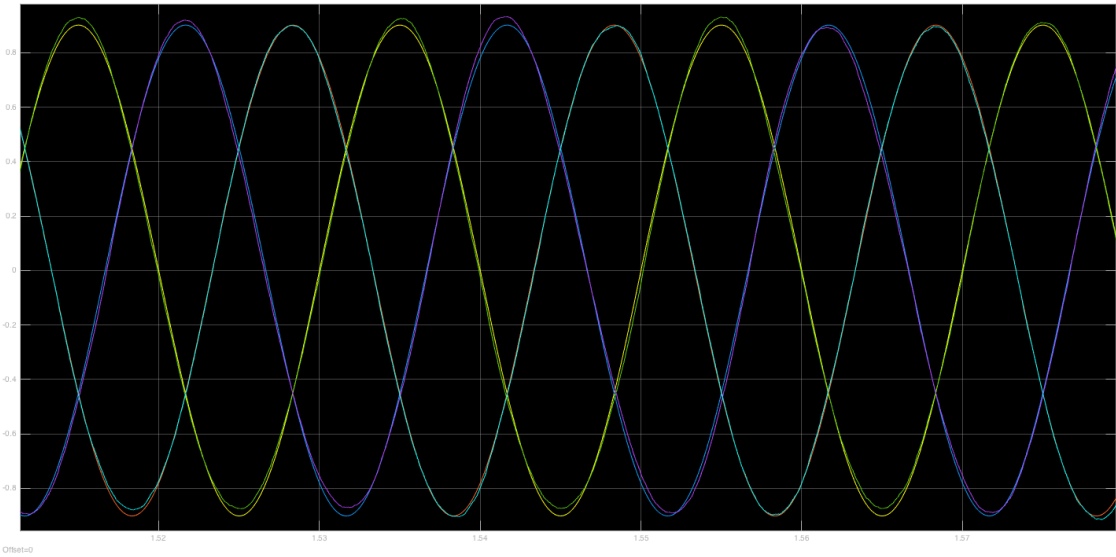


Figure 6.14: Voltages driving grid currents in pu.

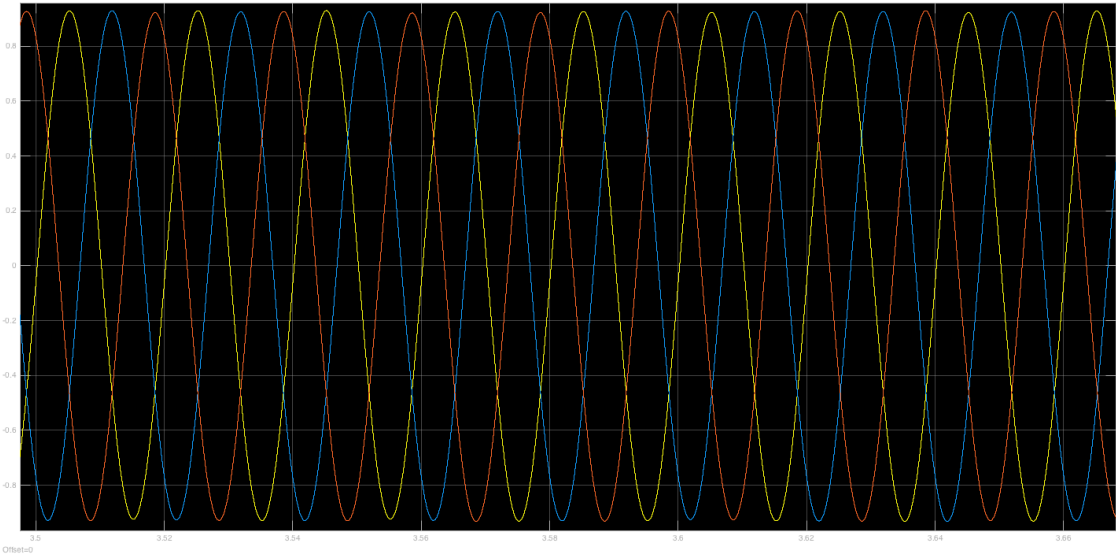


Figure 6.15: Voltages driving grid currents in pu.

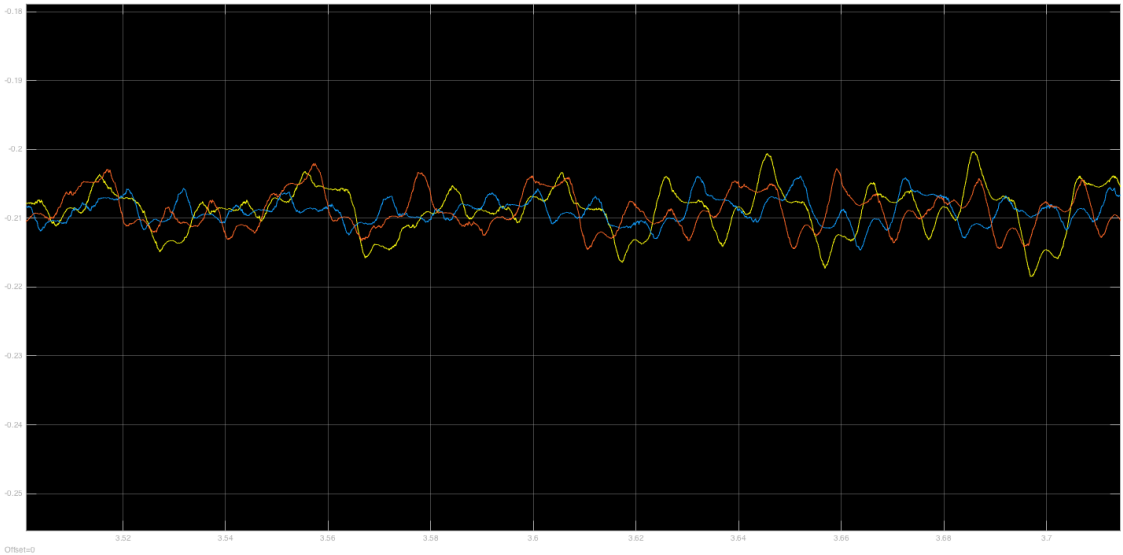


Figure 6.16: Voltage driving the circulating current before the PI control.

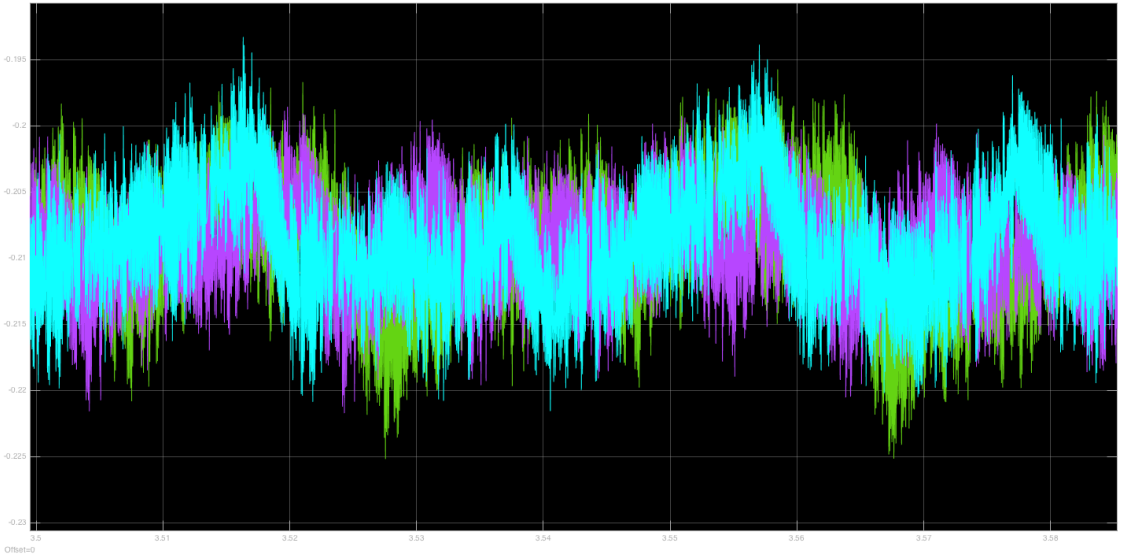


Figure 6.17: Voltage driving the circulating current after the PI control.

6.5 Simulation of IFOC for PMSG interfaced with two-level inverter

Following section will contain a brief explanation of the simulation and obtained results. The results used in this section are adopted from the project report that was done by the student during master studies. [42] The initialization process lasts 1 sec. At $t=1.2$ sec the machine is given a ramp speed reference in no load ($T_m=0$). This reference creates the q-axis reference and as a result the electromagnetic torque that speeds up the machine. Here, since $T_m=0$, the machine is controlled as being a motor. The Simulation results are shown in the Figure 6.19. It must be mentioned that both the initialization process and the resting time before giving the speed reference, should be longer to assure that the rotor is still and there are no currents flowing. [42]

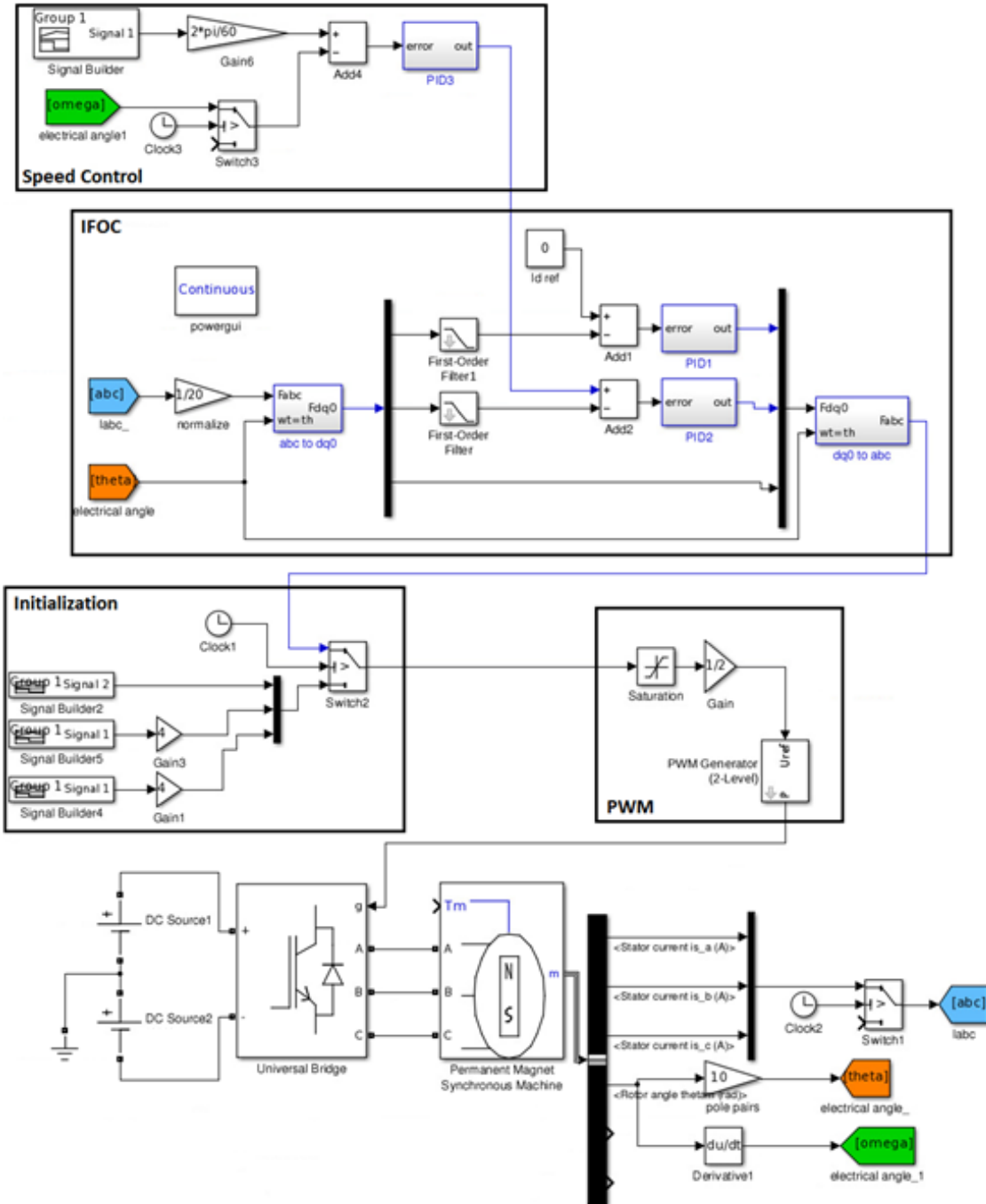


Figure 6.18: PMSG with two level inverter. Speed regulator and indirect field oriented control [42].

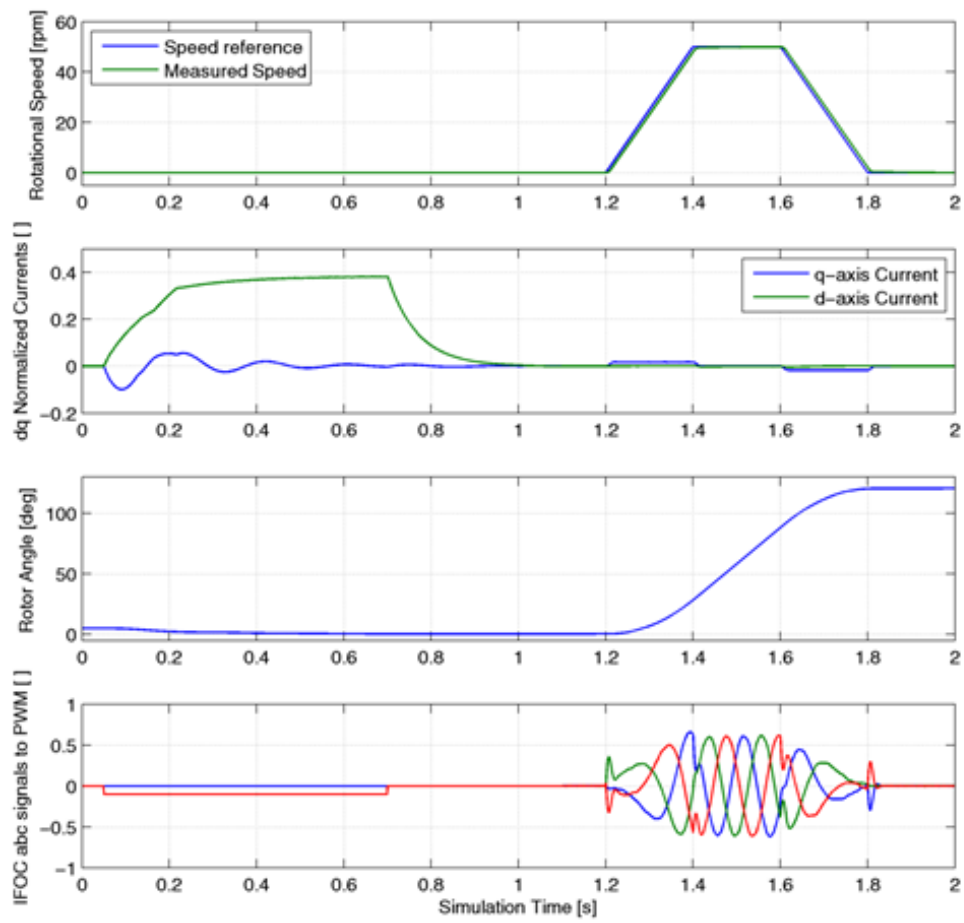


Figure 6.19: d-q axes currents and torque regulation [42].

Discussion. Conclusion. Future work

The process of the design of two different wind energy electrical systems, such as interfaced with two-level back-to-back voltage-source inverter and back-to-back MMC, has many differences. The two-level inverter is more simple topology and in this way it is easier to design the control and calculated parameters for the semiconductor components. On the other hand it is very popular and very often is described in the literature, so in nearest future there is a high chance of increase of the interest of MMC for Wind Energy applications. During the design and simulation process of the wind energy system interfaced with back-to-back MMC several complications appeared:

- The control of the generator side MMC is complex and hard to implement.
- The evaluation of the results deteriorates because of the high number of iterations that slow down simulations, 5 second simulation of the complete 11-level model with back-to-back MMC was running approximately 12 hours in Accelerator mode. Author suggests to use supercomputer for future simulations and analysis.
- Simulation model contains a high number of control levels that make the tuning process slow and complex.

Development of different Wind Energy systems for high power applications is vital question in modern wind turbine studies. Wind Turbines become bigger and require new more reliable, safe and efficient solutions. Future studies of MMC implementation for large-scale wind turbines should be carried out.

Unfortunately this master thesis is not highlighting all the different sides of MMC implementation and the obtained results can not be evaluated as final. In the future it is necessary to run the simulation using more powerful tools, for example super-computer, so the scope of simulation will be able to highlight more detailed simulation structure, for example operation under unstable wind conditions.

For the future work it is also suggested to perform an energy analysis of the MMC semiconductor components, like diodes, IGBT's, inductors and capacitors to check the energy dynamics. Also more detailed harmonic analysis should be performed.

References

- [1] GWEC Global Wind Energy Council. Wind in numbers, 2015. URL <http://www.gwec.net/global-figures/wind-in-numbers/>.
- [2] L. Popova, J. Pyrhonen, K. Ma, and F. Blaabjerg. Device loading of modular multilevel converter mmc in wind power application. In *Power Electronics Conference (IPEC-Hiroshima 2014 - ECCE-ASIA), 2014 International*, pages 548–554, May 2014. doi: 10.1109/IPEC.2014.6869638.
- [3] Gilbert Bergna Diaz. *Modular Multilevel Converter Control for Multi-Terminal HVDC Operation*. PhD thesis, Sintef, September 30, 2014.
- [4] G. Bergna, J.C. Vannier, P. Lefranc, A. Arzande, E. Berne, P. Egrot, and M. Molinas. Modular multilevel converter leg-energy controller in rotating reference frame for voltage oscillations reduction. In *Power Electronics for Distributed Generation Systems (PEDG), 2012 3rd IEEE International Symposium on*, pages 698–703, June 2012. doi: 10.1109/PEDG.2012.6254078.
- [5] G. Bergna, E. Berne, P. Egrot, P. Lefranc, J.-C. Vannier, A. Arzande, and M. Molinas. Modular multilevel converter-energy difference controller in rotating reference frame. In *Power Electronics and Motion Control Conference (EPE/PEMC), 2012 15th International*, pages LS2c.1–1–LS2c.1–4, Sept 2012. doi: 10.1109/EPEPEMC.2012.6397413.
- [6] 2014 marked a record year for global wind power, . URL <http://www.gwec.net/global-figures/wind-energy-global-status/>.
- [7] Market forecast for 2015-2019, . URL <http://www.gwec.net/global-figures/market-forecast-2012-2016/>.
- [8] Shimon Awerbuch Sren Krohn (editor), Poul-Erik Morthorst. The economics of wind energy. a report by the european wind energy association, March 2009.
- [9] Donald L. Fike Ica Manas-Zloczower Usama Younes Serkan Unal Peter Emrich Frank Bradish Richard SESCO Marcio R. Loos, Cristimari R. O. Loos. Worlds first carbon

- nanotube reinforced polyurethane wind blades. URL <http://engineering.case.edu/emacs/news/Carbon-Nanotube-Reinforced>.
- [10] Martin O. L. Hansen. *Aerodynamics of Wind Turbines*. London. Earthscan, 2 edition, 2008.
 - [11] Bogi Bech Jensen. *Lecture slides for the course Wind Turbine Electrical Design*. Technical University of Denmark, Anker Engelunds Vej 1 Bygning 101A, 2800 Kgs. Lyngby, Denmark, sep 2013.
 - [12] F. Senani, F. Louar, M. Boulkenefet, and H. Benalla. Wind conversion chain model simulation using pi controler for voltage regulation. In *Renewable Energy Congress (IREC), 2014 5th International*, pages 1–5, March 2014. doi: 10.1109/IREC.2014.6826994.
 - [13] power technology.com. Egmond aan zee offshore wind farm, netherlands. vestas v90-3.0 turbine., nov 2015. URL <http://www.power-technology.com/projects/egmond/egmond4.html>.
 - [14] Navid Zargari Samir Kouro Bin Wu, Yongqiang Lang. *Power Conversion and Control of Wind Energy Systems*. John Wiley Sons, Inc., Hoboken, New Jersey, 2011.
 - [15] H. Polinder. Overview of and trends in wind turbine generator systems. In *Power and Energy Society General Meeting, 2011 IEEE*, pages 1–8, July 2011. doi: 10.1109/PES.2011.6039342.
 - [16] Xu Yang, D. Patterson, and J. Hudgins. Permanent magnet generator design and control for large wind turbines. In *Power Electronics and Machines in Wind Applications (PEMWA), 2012 IEEE*, pages 1–5, July 2012. doi: 10.1109/PEMWA.2012.6316367.
 - [17] E.de Vries Dr Z. Chen M Mueller, H Polinder. Electrical drives for direct drive renewable energy systems. *Woodhead Publishing Series in Energy*, 24:106–156, 2013.
 - [18] Long Pham. A review of full scale converter for wind turbines. page 8. URL https://www.academia.edu/5759035/A_Review_of_Full_Scale_Converter_for_Wind_Turbines.
 - [19] F. Blaabjerg, F. Iov, Z. Chen, and K. Ma. Power electronics and controls for wind turbine systems. In *Energy Conference and Exhibition (EnergyCon), 2010 IEEE International*, pages 333–344, Dec 2010. doi: 10.1109/ENERGYCON.2010.5771701.
 - [20] Ned Mohan, Tore M. Undeland, and William P. Robbins. *Power Electronics. Converters, Applications and Design*. John Wiley and Sons, Inc, third edition, 2003.
 - [21] Nantao Huang. Simulation of power control of a wind turbine permanent magnet synchronous generator system. Master’s thesis, Marquette University, 2013. URL http://epublications.marquette.edu/theses_open/215/.
 - [22] J. C. Kingsley A. E. Fitzgerald and S. D. Umans. *Electric Machinery*. New York: McGraw-Hill, 1990.

- [23] A. Lesnicar and R. Marquardt. An innovative modular multilevel converter topology suitable for a wide power range. In *Power Tech Conference Proceedings, 2003 IEEE Bologna*, volume 3, pages 6 pp. Vol.3–, June 2003. doi: 10.1109/PTC.2003.1304403.
- [24] Wikipedia. The free encyclopedia. HvdC converter, jan 2015. URL https://en.wikipedia.org/wiki/HVDC_converter.
- [25] P.S. Jones and C.C. Davidson. Calculation of power losses for mmc-based vsc hvdc stations. In *Power Electronics and Applications (EPE), 2013 15th European Conference on*, pages 1–10, Sept 2013. doi: 10.1109/EPE.2013.6631955.
- [26] G.P. Adam, K.H. Ahmed, and B.W. Williams. Mixed cells modular multilevel converter. In *Industrial Electronics (ISIE), 2014 IEEE 23rd International Symposium on*, pages 1390–1395, June 2014. doi: 10.1109/ISIE.2014.6864817.
- [27] Lennart Angquist, A. Antonopoulos, D. Siemaszko, K. Ilves, M. Vasiladiotis, and H.-P. Nee. Open-loop control of modular multilevel converters using estimation of stored energy. *Industry Applications, IEEE Transactions on*, 47(6):2516–2524, Nov 2011. ISSN 0093-9994. doi: 10.1109/TIA.2011.2168593.
- [28] J.A. Martinez-Velasco. *Transient Analysis of Power Systems: Solution Techniques, Tools and Applications*. Wiley - IEEE. Wiley, 2014. ISBN 9781118694176. URL <https://books.google.se/books?id=7eOfBQAAQBAJ>.
- [29] D. Jovcic and K. Ahmed. *High Voltage Direct Current Transmission: Converters, Systems and DC Grids*. Wiley, 2015. ISBN 9781118846681. URL <https://books.google.se/books?id=2fI-CgAAQBAJ>.
- [30] M. Zygmanowski, B. Grzesik, and R. Nalepa. Capacitance and inductance selection of the modular multilevel converter. In *Power Electronics and Applications (EPE), 2013 15th European Conference on*, pages 1–10, Sept 2013. doi: 10.1109/EPE.2013.6634446.
- [31] C. Busca, A.-I. Stan, T. Stanciu, and D.I. Stroe. Control of permanent magnet synchronous generator for large wind turbines. In *Industrial Electronics (ISIE), 2010 IEEE International Symposium on*, pages 3871–3876, July 2010. doi: 10.1109/ISIE.2010.5637628.
- [32] Victor M. F. Mendes Rui Melcio and Joo P. S. Catalo. *Wind Turbines*, chapter Wind Turbines with Permanent Magnet Synchronous Generator and Full-Power Converters: Modelling, Control and Simulation. InTech, 2011.
- [33] Nantao Huang. Simulation of power control of a wind turbine permanent magnet synchronous generator system. Master’s thesis, Marquette University, 2009.
- [34] F. Blaabjerg and Ke Ma. Future on power electronics for wind turbine systems. *Emerging and Selected Topics in Power Electronics, IEEE Journal of*, 1(3):139–152, Sept 2013. ISSN 2168-6777. doi: 10.1109/JESTPE.2013.2275978.
- [35] Radu Ghiga. Experimenting with flexible vector control schemes for wind turbine generators. digital field-oriented control. Master’s thesis, Technical University of Denmark, sep 2013.

- [36] J.I. Leon, S. Vazquez, J.A. Sanchez, R. Portillo, L.G. Franquelo, J.M. Carrasco, and E. Dominguez. Conventional space-vector modulation techniques versus the single-phase modulator for multilevel converters. *Industrial Electronics, IEEE Transactions on*, 57(7):2473–2482, July 2010. ISSN 0278-0046. doi: 10.1109/TIE.2009.2034674.
- [37] N. Celanovic and D. Boroyevich. A fast space-vector modulation algorithm for multilevel three-phase converters. *Industry Applications, IEEE Transactions on*, 37(2): 637–641, Mar 2001. ISSN 0093-9994. doi: 10.1109/28.913731.
- [38] Yi Deng, Yebin Wang, Koon Hoo Teo, and R.G. Harley. Space vector modulation method for modular multilevel converters. In *Industrial Electronics Society, IECON 2014 - 40th Annual Conference of the IEEE*, pages 4715–4721, Oct 2014. doi: 10.1109/IECON.2014.7049213.
- [39] prof. Robert Nilssen Hilde Evensen Liseth. 10 mw reference wind turbine. *Department of Electrical Engineering, NTNU*, page 9, 2015.
- [40] H. Polinder, D. Bang, R.P.J.O.M. van Rooij, A.S. McDonald, and M.A. Mueller. 10 mw wind turbine direct-drive generator design with pitch or active speed stall control. In *Electric Machines Drives Conference, 2007. IEMDC '07. IEEE International*, volume 2, pages 1390–1395, May 2007. doi: 10.1109/IEMDC.2007.383632.
- [41] G. Shrestha J.A. Ferreira D. Bang, H. Polinder. Review of generator systems for direct-drive wind turbines. *Electrical Power Processing / DUWIND, Delft University of Technology*, page 11, 2007.
- [42] Rizwan R. Syed Dimitrios Panagiotopoulos, Kateryna Morozovska. Project report

Appendix A

Calculation of converter parameters

```
1 %%Sizing of MMC
2
3 %initial parameters
4 Vacll      =3300;    % V
5 DCgain      =2;      % AC to DC gain
6 Nsm         =2;      % number of submodules in each arm
7 epsilon     =0.1;    % ripple
8 P           =10e6;    % MW
9 Q           =3.5e6;    % MVA
10 cosphi      =0.999999; % power factor
11 f           =50;     % Hz
12 k           =1;
13 deltaT      =40e-6;  % s fault detection time
14 n_cells_arm =10;
15 rho=1.225; %kg/m
16 R=154/2;
17
18 Tt=40e-6;
19 omega       =2*pi*f; %
    angular frequency
20 Vacrms      =Vacll*sqrt(2)/sqrt(3);
21 Vdc         =Vacrms*DCgain;
22 Vsm         =Vdc/Nsm;
23 phi         =acos(cosphi);
24 V_DC=Vdc;
25 Pgen        =P*1.06; %
    MW (P+6%)
26 S           =sqrt(Q^2+Pgen^2); %
    MVA
27 deltaWsm    =2/3*S/k/omega/Nsm*(1-(k*cosphi/2)^2)^(1.5);
```

```

28
29 %Sub module capacitance
30 Csm      =deltaWsm/2/epsilon/Vsm^2;
31
32 %Circulating current
33 Ic       =Pgen^(3*phi)/3/Vdc;
34 deltaIc  =0.2*Ic;
35
36 %Arm inductance
37 Larm     =Vdc*deltaT/2/deltaIc;
38
39 C=Csm;
40 Kp=1;
41 Kl=0.5;
42 IBASE=15;
43 rho=1.225; %kg/m
44 R=154/2;

```

Appendix B

Balancing algorithm for one arm of the converter

```
1 function y = fcn(u, iabc, c)
2 %#codegen
3 m=round(c);
4 s=size(u);
5 y=[0;0;0;0;0;0;0;0;0;0;0];
6 i=1;
7 k=size(u);
8 for i=1:10
9     if m==0;
10         a = zeros(s(1),1);
11     elseif m==s(1);
12         a = ones(s(1),1);
13     else
14         [y,I] = sortrows(u);
15
16         if iabc >= 0
17             a = zeros(s(1),1);
18             q = I(1:m);
19             a(q,1)=1;
20         else
21             a = ones(s(1),1);
22             q = I(1:s(1)-m);
23             a(q,1)=0;
24         end
25     end
26     y(i)=a(i);
27     i=i+1;
28 end
```

Appendix C

Space Vector Modulation script

```
1 function [v1,v2,d1,d2] = fcn(u,N)
2 %#codegen
3
4 a = floor(u);
5
6     v1 = a;
7     v2 = a+1;
8     d2 = u - a;
9     d1 = 1-d2;
10
11
12 function [y,V1OLD,V2OLD,D1OLD,D2OLD,z] = fcn(v1,v2,d1,d2,v1old,
13     v2old,d1old,d2old,t,tsvm,yold)
14 %#codegen
15 tol = 0;
16
17 V1OLD = v1old;
18 V2OLD = v2old;
19 D1OLD = d1old;
20 D2OLD = d2old;
21
22 if abs(t) <= tol
23     v1x = v1;
24     v2x = v2;
25     d1x = d1;
26     d2x = d2;
27
28     V1OLD = v1;
29     V2OLD = v2;
30     D1OLD = d1;
```

```
30     D2OLD = d2;
31 else
32
33
34     v1x = v1old;
35     v2x = v2old;
36     d1x = d1old;
37     d2x = d2old;
38
39
40 end
41
42 if t>0 && t-d1x*tsvm<0
43     y=v1x;
44     z=1;
45 elseif t -tsvm < 0 && t-tsvm*(1-d2x)>0
46     y=v2x;
47     z=0;
48 elseif t==0
49     y=v1x;
50     z=3;
51 elseif t == d1x*tsvm || t== tsvm*(1-d2x)
52     y=v2x;
53     z=2;
54 elseif t== tsvm
55     y = v2x;
56     z=5;
57 else
58     y=yold;
59     z=8;
60 end
```